

LiU-ITN-TEK-A--08/122--SE

# Detection of annual rings in wood

Christian Jonsson

2008-11-14



**Linköpings universitet**  
**TEKNISKA HÖGSKOLAN**

LiU-ITN-TEK-A--08/122--SE

# **Detection of annual rings in wood**

Examensarbete utfört i medieteknik  
vid Tekniska Högskolan vid  
Linköpings universitet

**Christian Jonsson**

Handledare Claes Nelsson  
Examinator Björn Kruse

Norrköping 2008-11-14

## Upphovsrätt

Detta dokument hålls tillgängligt på Internet – eller dess framtida ersättare – under en längre tid från publiceringsdatum under förutsättning att inga extra-ordinära omständigheter uppstår.

Tillgång till dokumentet innebär tillstånd för var och en att läsa, ladda ner, skriva ut enstaka kopior för enskilt bruk och att använda det oförändrat för ickekommersiell forskning och för undervisning. Överföring av upphovsrätten vid en senare tidpunkt kan inte upphäva detta tillstånd. All annan användning av dokumentet kräver upphovsmannens medgivande. För att garantera äktheten, säkerheten och tillgängligheten finns det lösningar av teknisk och administrativ art.

Upphovsmannens ideella rätt innefattar rätt att bli nämnd som upphovsman i den omfattning som god sed kräver vid användning av dokumentet på ovan beskrivna sätt samt skydd mot att dokumentet ändras eller presenteras i sådan form eller i sådant sammanhang som är kränkande för upphovsmannens litterära eller konstnärliga anseende eller egenart.

För ytterligare information om Linköping University Electronic Press se förlagets hemsida <http://www.ep.liu.se/>

## Copyright

The publishers will keep this document online on the Internet - or its possible replacement - for a considerable time from the date of publication barring exceptional circumstances.

The online availability of the document implies a permanent permission for anyone to read, to download, to print out single copies for your own use and to use it unchanged for any non-commercial research and educational purpose. Subsequent transfers of copyright cannot revoke this permission. All other uses of the document are conditional on the consent of the copyright owner. The publisher has taken technical and administrative measures to assure authenticity, security and accessibility.

According to intellectual property law the author has the right to be mentioned when his/her work is accessed as described above and to be protected against infringement.

For additional information about the Linköping University Electronic Press and its procedures for publication and for assurance of document integrity, please refer to its WWW home page: <http://www.ep.liu.se/>

## Abstract

This report describes an annual line detection algorithm for the WoodEye quality control system. The goal with the algorithm is to find the positions of annual lines on the four surfaces of a board. The purpose is to later use this result together with an existing algorithm to find the inner annual ring structure of the board. The work was done using image processing techniques to analyze images collected with WoodEye.

The report gives the reader an insight in the requirements of quality control systems in the woodworking industry and the benefits of automated quality control versus manual inspection. The appearance and formation of annual lines are explained on a detailed level to provide insight on how the problem should be approached.

A comparison between annual rings and fingerprints are made to see if ideas from this area of pattern recognition can be adapted to annual line detection. This comparison together with a study of existing methods led to the implementation of a fingerprint enhancement method. This method became a central part of the annual line detection algorithm.

The annual line detection algorithm consists of two main steps; enhancing the edges of the annual rings, and tracking along the edges to form lines.

Different solutions for components of the algorithm were tested to compare performance. The final algorithm was tested with different input images to find if the annual line detection algorithm works best with images from a grayscale or an RGB camera.

## Preface

This thesis project was carried out as a part of the Media Technology program at the department of Science and Technology, Linköping University. It was performed during the period 11/2007- 06/2008 in cooperation with Innovativ Vision AB. The project was carried out under supervision of Senior Researcher Claes Nelsson at Innovativ Vision AB in Linköping.

During this project I have learnt a lot about problem solving, programming in Matlab and image processing, and last but not least, a whole lot about wood and how it is processed. Many of these new insights came from analyzing, solving or working around problems I encountered. But others have come just from spending time with people in the industry, listening and asking questions.

I would like to thank my supervisor Claes Nelsson for his guidance, support and patience. Many thanks go to PhD Maria Magnusson for the valuable help with the adaptation of the fingerprint algorithm. My gratitude goes to all the people at Innovativ Vision AB who helped me and contributed to making my stay there a pleasant experience. Thanks also go to my examiner Professor Björn Kruse.

## List of figures

Figure 1: The inner annual ring structure of two board crossections .....	2
Figure 2: WoodEye.....	3
Figure 3: Annual lines of a board.....	6
Figure 4: Fingerprint image .....	7
Figure 5: The density is related to the darkness of the wood.....	9
Figure 6(a) and (b): These annual lines are easy to identify even from an intensity profile.....	10
Figure 7(a) and (b): The annual lines here are harder to separate from noise and color variations .....	10
Figure 8: A sawn board .....	11
Figure 9: The axes of a tree .....	12
Figure 10: A high level overview of the ALD algorithm.....	16
Figure 11: The FPE algorithm.....	17
Figure 12: The Sobel operators .....	18
Figure 13: The intensity of the gradient rises and falls as it describes the lines .....	19
Figure 14: Direction of edges .....	20
Figure 15: The result of changing $fx$ from positive to negative .....	20
Figure 16: The effect of doubling the directional angles of a line .....	21
Figure 17: After doubling the angle, a light-dark edge will have the same direction as a dark-light edge... 21	
Figure 18(a): An edge described as a vector of its derivatives $fx$ and $fy$ .....	22
Figure 19: A 1D description of the derivative in double angle representation.....	23
Figure 20: The final FPE algorithm .....	24
Figure 21: An image of a board section, before it has been processed by the FPE algorithm.....	25
Figure 22: The same board section, after being processed by the FPE algorithm .....	25
Figure 24: Here, the L-E transitions are a lot more distinct than the E-L transitions .....	26
Figure 23: The ALD algorithm .....	26
Figure 25: An intensity profile .....	27
Figure 26: The gradient profile .....	28
Figure 27: The annual lines to the left are wider than those to the right.....	29
Figure 28: A gradient profile of the board in Figure 27 .....	30
Figure 29: The slope of the curve shows that the pith is located somewhere to the left of this board.....	30
Figure 31: The lines on the up and down side of the board has grown in opposite directions .....	31
Figure 30: The location of the pith .....	31
Figure 32(a): k-3.....	32

Figure 33: Vertical correction .....	33
Figure 34: Horizontal correction.....	34
Figure 35: Path collision .....	35
Figure 36: Piecewise segmentation .....	37
Figure 37: The final ALD algorithm .....	37
Figure 38: Test sample 1 .....	38
Figure 39: Test sample 2 .....	39
Figure 40: Test sample 3 .....	39
Figure 41: Test sample 4 .....	40
Figure 42: Test sample 5 .....	40
Figure 43: Test sample 6 .....	41
Figure 44: Test sample 7 .....	41
Figure 45: Test sample 8 .....	42
Figure 46: Line detection performed on all four sides of a board .....	43
Figure 47: Line detection performed on all four sides of a board .....	44

## Contents

1 Introduction.....	1
1.1 Outline .....	1
1.2 Purpose and goal.....	1
1.3 Limitations .....	1
1.4 Background .....	2
1.4.1 WoodEye.....	3
1.4.2 Fingerprints and annual rings – a comparison of patterns .....	5
1.4.3 Early wood and late wood .....	8
1.4.4 The visual appearance of wood .....	9
1.5 Terminology .....	11
1.6 Methodology.....	14
1.6.1 Literature study and evaluation of methods .....	14
2 Algorithm for detection of annual lines .....	16
2.1 Fingerprint enhancement.....	17
2.1.1 Edge detection and enhancement .....	18
2.1.2 Semi-global orientation .....	19
2.1.3 Double angle .....	21
2.1.4 Modifications .....	24
2.2 Determining the growth direction and finding the seed points .....	26
2.3 Linetracing .....	32
2.3.1 Linetracing vs. Binarization .....	36
2.4 Validation of lines.....	37
2.4.1 Piecewise segmentation .....	37
3 Results .....	38
3.1 Discussion .....	45
3.2 Tests .....	46
4 Conclusions.....	49
4.1 Future improvements.....	50
5 References .....	52
Appendix .....	53



# 1 Introduction

## 1.1 Outline

This report consists of four chapters. Chapter one, the introductory chapter, presents the purpose and the background information required to fully understand the reasoning behind different approaches in the development of the algorithm. The reader is introduced to quality assessment of wood, and to WoodEye, the scanner that this algorithm is developed for. This chapter also describes how the work was carried out. Chapter two gives a detailed overview of the implementation of the algorithm. In the third chapter, the results of the algorithm are discussed and image samples are presented together with comparative tests. Chapter four summarizes ideas and improvements of the algorithm.

## 1.2 Purpose and goal

The goal of this work is to develop an algorithm that from images acquired with the WoodEye scanner system finds the positions of annual rings on the four sides of a board. The purpose is to later use this result together with an existing annual ring analyzer algorithm to find the inner annual ring structure of the board. The input to the analyzer algorithm is the positions of annual rings on all four sides of a board within the same longitudinal coordinate. This means that it is sufficient to detect annual rings on a single one pixel wide board profile. The algorithm described in this report will for reasons explained later detect annual rings on board segments of arbitrary length.

The algorithm must be fully automated and be able to analyze boards with varying appearances. The speed is also very important since the algorithm is to be integrated in to WoodEye which runs in full production speed up to 650 meters/minute. A part of the assignment has been to search for, and study documented methods of annual ring analysis to see if any of the existing methods are suitable for adaptation for WoodEye. The goal is to establish the positions of the annual lines on a given longitudinal coordinate, on all four sides of a board.

## 1.3 Limitations

The character of annual rings varies greatly between different kinds of wood, and finding a method that can handle all of them requires an extensive amount of work and research, not fitting into the limits of a thesis project. This method is therefore adapted, but not limited, to boards of spruce. The reason spruce was chosen is that this is the most common type of wood in the Swedish wood industry, and also the most important type of construction wood.

Among softwood, spruce is considered one of the most difficult types to determine annual rings from. This is due to the low contrast between early and late wood. Since the characteristics of annual rings are quite similar within the softwood group, one can say that if the algorithm can detect annual rings for spruce, it will be able to detect the annual rings for most other softwood as well.

The input image to the algorithm is preprocessed by WoodEye in order to provide a defect-free section. This is of great benefit since the character of the line pattern is disturbed near defects like knots and rot. Many of the conclusions drawn about line patterns in this report are made on the basis of a defect-free board section.

## 1.4 Background

A higher competition in the woodworking industry is constantly forcing the production speed to increase, while at the same time maintaining or increasing the quality of the output. Quality assessment and pricing rely largely on the visual appearance of the surface, where boards are classified by the occurrence of different defects. For this reason, visual inspection and sorting is an important issue for the sawmill. A trained eye can, by inspecting the board surface, estimate the quality based on predetermined rules and classes. But a modern automated quality control system is faster, more accurate and more consistent than any human eye can ever be. By achieving a more consistent and accurate grading, and providing the customer with the quality he wants, less revenue will be lost due to under grading, and fewer customers will be dissatisfied due to over grading.

An important part of quality assessment of wood is to know the positions of the annual rings. Knowing the positions on the surface provides information about the aesthetic appearance, but more importantly, it is the basic requirements for determining the inner annual ring structure (the pattern of annual rings of a board cross section). The distance between annual rings in the inner structure provides important parameters for the estimation of the strength of the wood. Knowing if the inner annual ring structure is standing (vertical) or lying (horizontal) provides information about how resistant the wood is to rot and cracks and how the wood can be used, see Figure 1. The ability to detect and position annual rings are therefore of great benefit to an automated quality control system.

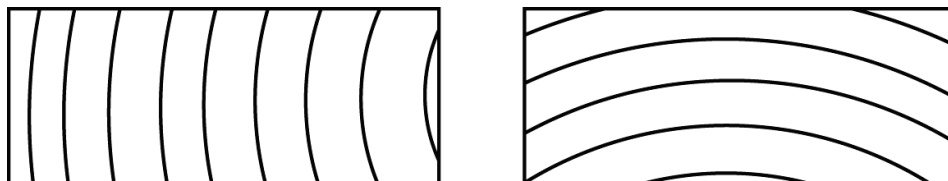


Figure 1: The inner annual ring structure of two board crossections. The board to the left as a standing inner structure. The board to the right has a lying inner structure.

To analyze annual ring patterns, systems like *Argus Frontal* [8] or the *Sprescan Ring series* [9] scan the cross-section of the boards. This requires a separate station since the boards need to be transported transversally. By analyzing the annual ring pattern on the board surface instead of the cross-section, the algorithm can run on any standard longitudinal feed scanner without the requirement of additional hardware or directional change in the board transport. The direct information received from a longitudinal surface scan naturally differs from a cross-section scan, but the same information can eventually be extracted.

#### 1.4.1 WoodEye [7] [10]

Innovativ Vision AB is the company behind WoodEye. From 1983, 20 years of development have lead to what now is the 4<sup>th</sup> generation of WoodEye which is the market leader of quality control systems in the woodworking industry.

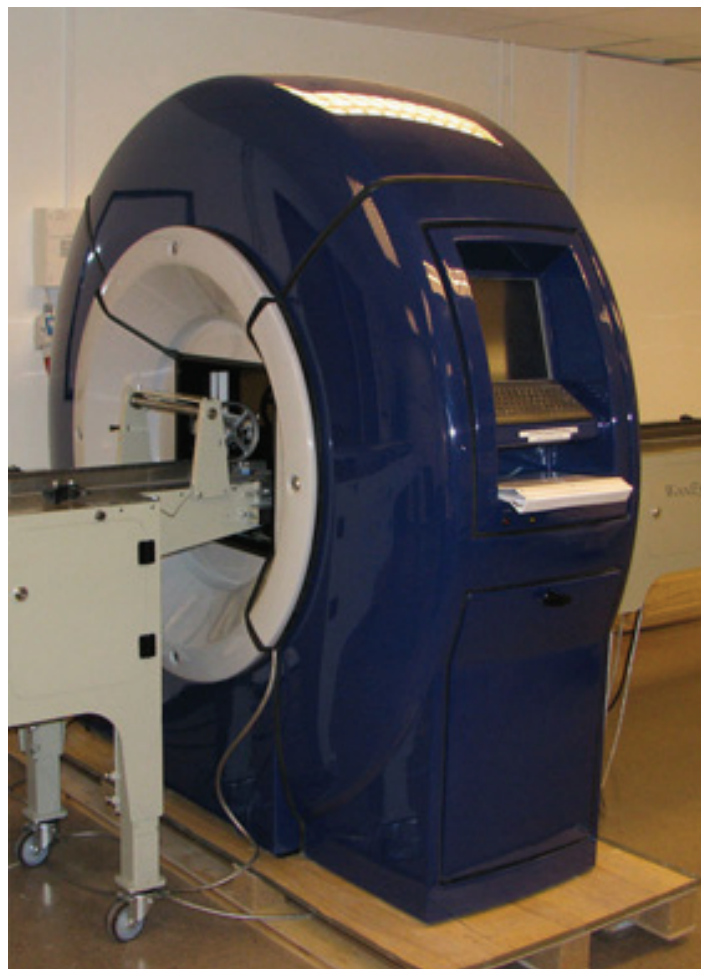


Figure 2: WoodEye

WoodEye is a scanner for sawn or planed wood. Boards are fed longitudinally through the scanner opening at full production speed. Inside the scanner there are a number of sensors. The setup and configuration of these sensors depend on the need of each individual customer. While WoodEye are capable of scanning all four sides of a board, a certain customer may for example only require sensors to scan two sides. WoodEye can be set up with several different kinds of advanced sensors, like high-resolution RGB or grayscale cameras, lasers or external sensors like moisture meters. These sensors detect any kind of defect, for example knots, cracks, rot and dimensional errors.

Not only the hardware comes in different configurations, the software is highly customizable and comes in different application specific packages.

- **WoodEye Sorter**  
Sorts the boards into quality classes according to the customer preset rules for the distribution of various defects. Each side of the board can be classified separately to maximize the yield.
- **WoodEye CrossCut**  
Optimizes cutting by comparing each inspected board to a reference list of all products in the production line. This list contains the number of components being produced, and the value and quality class requirement of each component. Each side of the board can be classified separately.
- **WoodEye Rip**  
This model has a wider opening and can take boards up to 750 mm wide [10]. WoodEye Rip optimizes in two dimensions, ripping (longitudinal cutting) and (cross-) cutting. It scans and classifies the up and down side of the board.
- **WoodEye Parquet & Flooring**  
In addition to detection of regular defects, WoodEye Parquet & Flooring also sorts by aesthetic criteria like texture and color. This scanner is tailor-made for parquet and flooring manufacturers.

These WoodEye models are further divided into customer specific versions, like for manufacturers of furniture, window frames or construction wood. The performance varies with the application, a typical speed is 60-200 meters/minute (WoodEye Training manual [7]) but operating speeds up to 650 meters/minute are possible

WoodEye keeps statistics of the production, like the number of each component produced, and the amount of waste. The quality can be analyzed per supplier or shipment and give an overview of quality changes over time.

#### 1.4.2 Fingerprints and annual rings – a comparison of patterns

When looking for inspiration and ideas, a study of the existing literature on pattern recognition for the application area of annual rings was made. This area of research is rather small compared to the closely related field of fingerprint analysis which is highly topical and a fast moving field of research. A comparison was made to find out if there were enough similarities between these two patterns for an adaptation to be meaningful.

The result of this comparison shows that there are both significant similarities and differences. The differences can be *simplifying*, meaning that the difference in question works in favor for an adaptation and the algorithm can be simplified. A difference can also be *complicating*, which means that for the algorithm to work for an annual line pattern, changes or additions need to be made.

Annual lines are collected by image scanning. Fingerprints are gathered by inking the raised ridges or pressing the finger against a surface, providing direct contact only with the raised ridges. The contrast of fingerprint patterns depends largely on the way the fingerprint is collected, the method and equipment used plays a significant role, while the contrast of the annual rings is completely dependent on the wood itself. This means that the contrast of annual rings can never be guaranteed.

#### Conclusion 1

The width of an annual ring depends on the speed the tree has grown. On a good year, the tree will grow faster and the ring will be thicker. The distances between the lines correspond to the rate the tree has grown each year. Looking at a cross-section of a tree it is obvious that an annual ring may vary in thickness from another, but variations within a single ring are small. The same conclusion can be drawn for a board if the board is sawn straight and are of reasonably limited length. This means that a line will run parallel to its closest neighbors, as illustrated in Figure 3.

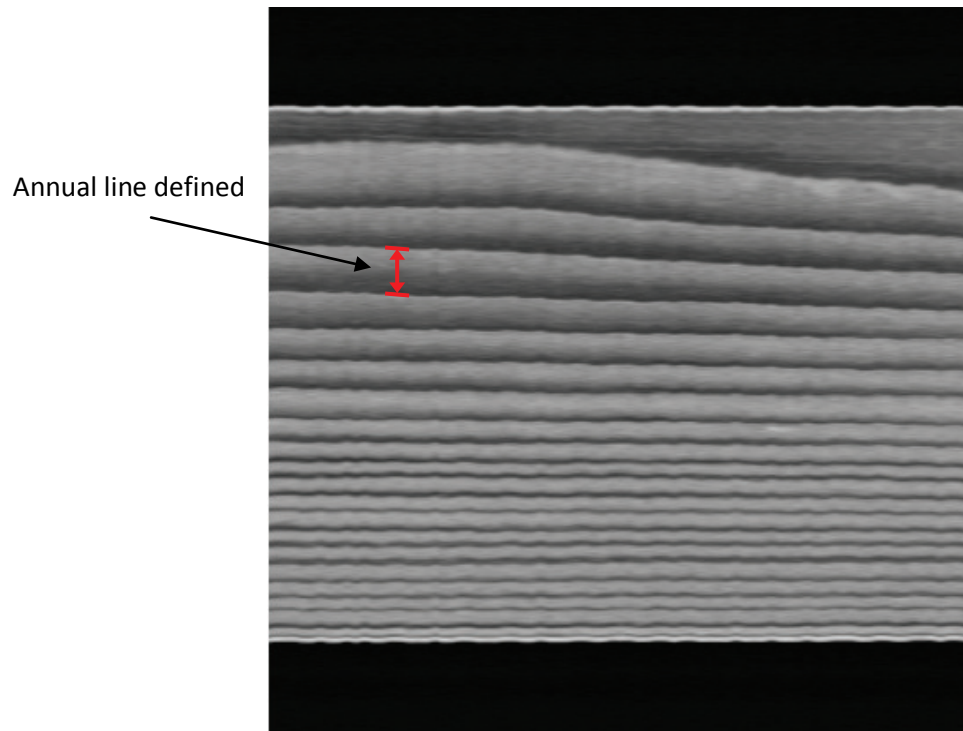


Figure 3: Annual lines of a board.

The distance between, and the width of ridges in a fingerprint image is approximately constant not only within a single line, but also within the whole fingerprint, as illustrated in Figure 4. Furthermore, the width does not differ much even from one fingerprint to another.



Figure 4: Fingerprint image. Courtesy of the Department of Electrical Engineering, Linköping University, MIPS [4].

**Conclusion 1 (a) (Similarity):**

*The width of a single line is fairly constant throughout the whole board-segment. A line will run parallel to its closest neighbors.*

**Conclusion 1 (b) (Complicating difference):**

*The annual lines on a board surface may vary in width between one another.*

**Conclusion 2**

The ridges in a fingerprint pattern has curvings in every possible angle, while the line pattern in wood has a very slow curving and rarely curve more than  $\pm 45^\circ$  from its general direction, which is along the long side of the board (the axial direction). This information can be used to greatly simplify the whole process - from edge detection to line segmentation.

**Conclusion 2 (Simplifying difference):**

*The line pattern on a board surface has a distinct axial main direction.*

**Conclusion 3**

Ridges in a fingerprint pattern will sometimes merge with another ridge, split in to 2 new ridges or suddenly end. Annual lines are always continuous and stop only at any of the edges of the board.

**Conclusion 3 (Simplifying difference):**

*The line pattern is continuous.*

**1.4.3 Early wood and late wood**

Annual rings can be perceived as streaks of brightness variations in the wood. These variations relate to the change in cell structure during the growth season of the tree. Early in the growing season during the spring, early wood is formed. Early wood has a light shade compared to the darker late wood that is formed during the summer, closer to the end of the growing season. The cells of early wood are larger and have thinner walls than those formed later in the season, this is because the dominant function of this newly formed wood is to transport water and nutrients up from the roots. The cells of late wood are smaller and have thicker walls to provide the tree with support. Late wood is harder, denser and stronger than early wood.



#### 1.4.4 The visual appearance of wood

The change in brightness in the radial direction ideally follows a ramp-model. In Figure 5, the wood has grown from left to right, forming the lighter early wood in the spring and gradually turning into the darker late wood until it stops growing in the end of the summer. The tree starts growing again in the spring next season, forming a visible contrast between late and early wood. This is what we perceive as the border between two annual rings. The darker the wood is the bigger is the ratio of smaller cells (late wood) with support as its dominant function. This means that density is related to the relative darkness of the wood.

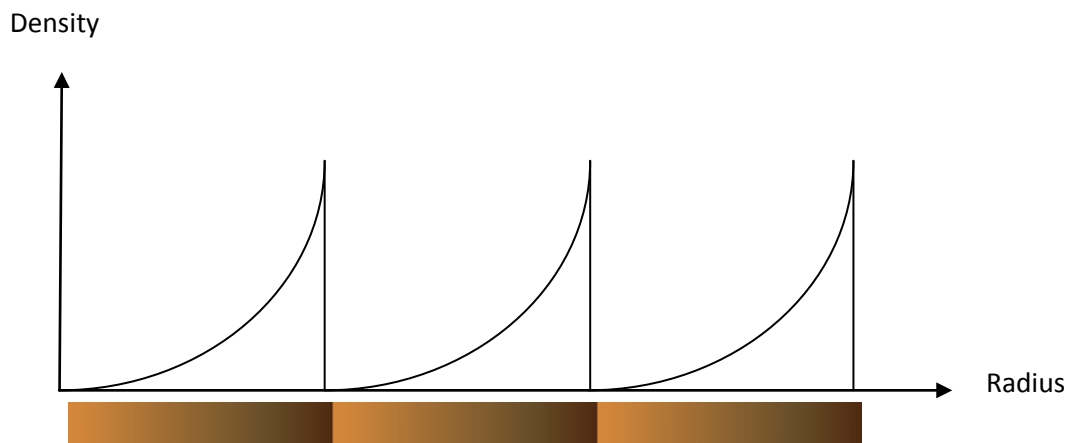


Figure 5: The density is related to the darkness of the wood. The slow increase of density represents the transition from early to late wood. The negative step illustrates the jump from late to early wood.

A 1D intensity profile following this model is shown in Figure 6(a), Figure 6(b) shows the board section the intensity information was taken from. Having the ramp-model in mind, it is possible to see with the bare eye that the wood has grown from left to right, and the pith of the tree has been somewhere to the left of the board. The graph shows the grayscale intensity, with the light shade as peaks and dark shade as valleys. Note that the ramps explained above are now flipped upside-down since this is an intensity plot, where a higher intensity corresponds to a lighter shade and a lower density.

It is easy to identify the annual lines from the intensity-plot in Figure 6(a), but it is rarely this clear, many times the plot will look something like in Figure 7(a). Here, the annual lines are hard to separate from noise, small cracks and other shade variations.

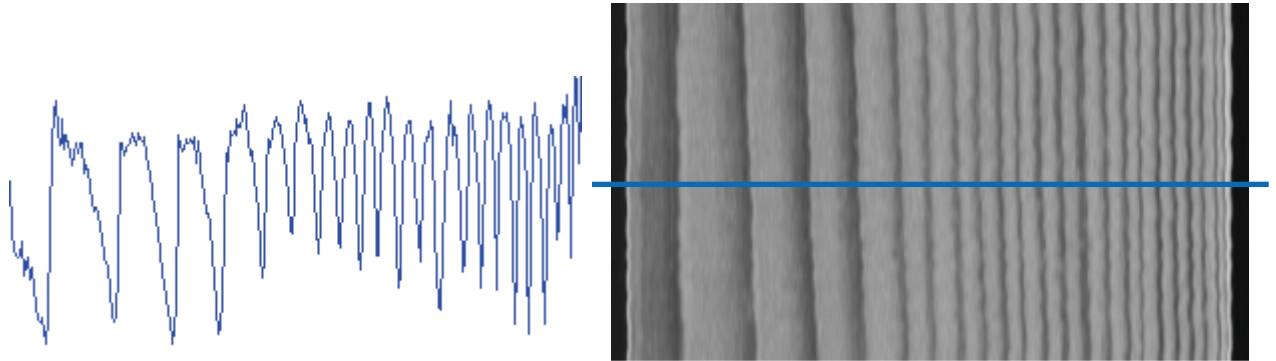


Figure 6(a) and (b): These annual lines are easy to identify even from an intensity profile.

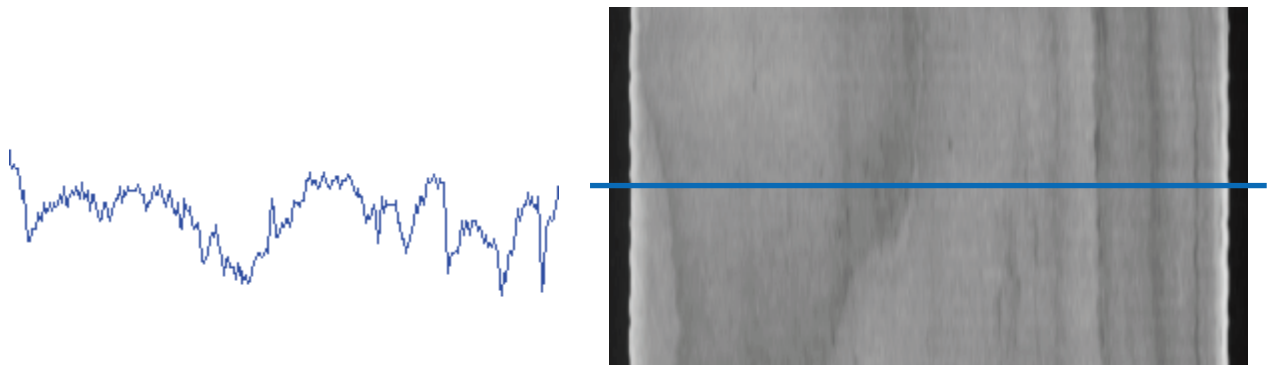


Figure 7(a) and (b): The annual lines here are harder to separate from noise and color variations.

On the basis of conclusion 1(b), annual lines are not always easy to identify from an intensity profile. An attempt to find the annual rings merely from an intensity profile would overlook a lot of helpful information like the priori knowledge about the direction of the pattern and the fact that it is continuous (see conclusion 3). A few pixels of discoloration or a small crack would be impossible to separate from the annual lines, while there would not be a big problem to rule them out from a 2D image.

## 1.5 Terminology

To simplify explanations and to avoid confusion, some definitions in this report are abbreviated. These abbreviations and other important distinctions are explained in this chapter.

- *Annual rings/ring-pattern* is what you see on a radial cross-section of a tree. They run in the *tangential* direction of a tree and this is what we generally mean with *annual rings*

- *Lines/line-pattern* run in the *axial* direction, this is what you see when you look at any of the four long sides of a sawn board (see Figure 8). The lines of a board run perpendicular to the radial cross-section.

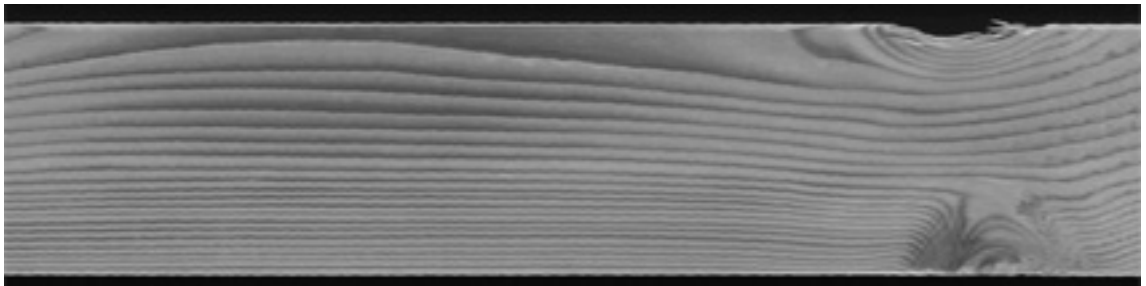


Figure 8: A sawn board.

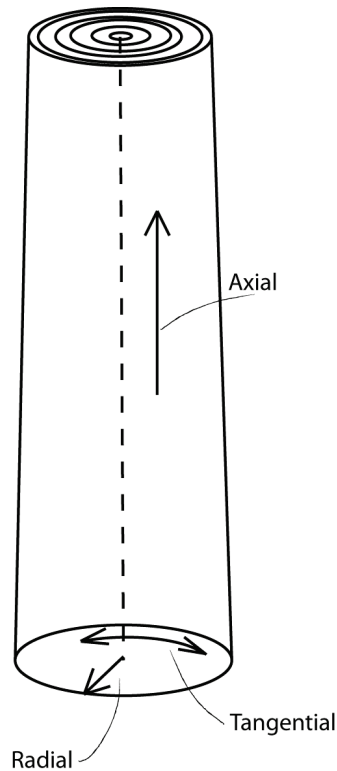


Figure 9: The axes of a tree

Some definitions used in this report:

<i>ALD algorithm</i>	The annual line detection algorithm described in this report.
<i>Board section</i>	A part of a board being examined by the ALD algorithm.
<i>Intensity profile/column</i>	A one pixel wide line, perpendicular to the long side of the board.
<i>FPE algorithm</i>	Fingerprint enhancement algorithm
<i>Out-image</i>	The resulting output image of the FPE algorithm.
<i>Line border</i>	The border between annual lines or rings.
<i>Line edge</i>	The edge response of a line border.
<i>Semi-global</i>	Larger than local, but not necessarily global.
<i>Linetrace/trace</i>	The process of growing a line by tracing along local maxima in an out-image.

<i>Pixel-path, path</i>	The one pixel wide line resulting from a trace.
<i>Line-buffer</i>	This is where all the valid pixel-paths are saved after the trace.
<i>Axial direction</i>	See Figure 9.
<i>Radial direction</i>	See Figure 9.
<i>Tangential direction</i>	See Figure 9.
<i>E-L response/signal</i>	Edge response caused by the transition from early wood to late wood.
<i>L-E response/signal</i>	Edge response caused by the transition from late wood to early wood.

## 1.6 Methodology

The work was divided in to four main phases;

- Literature study
- Evaluation of documented methods
- Development
- Documentation (this report)

### 1.6.1 Literature study and evaluation of methods

The purpose of the literature study was to look for existing methods of annual ring detection and to see if any of these could be adapted for WoodEye. Not a lot of work has been done in this particular area, but taking a look at a closely related field – fingerprint enhancement, significantly more documentation is available. Considering the similarities concluded in chapter 1.4.2, and that the research in this field is fast moving, fingerprint enhancement seemed like a good field to include in the literature study. In the evaluation phase, interesting methods found in the literature study was reviewed for consideration and compared.

Kellner et al. [5] look at annual lines on the surface of a board. They binarize the image by finding the local minima of each intensity profile in a grayscale image. This is done by fitting a parabola to the profile and finding the global minima for each interval of the profile located below, and bounded by, the parabola. The lines produced are then tracked using Dijkstra's algorithm.

Kellner [5] does not binarize or segment based on edge responses but on the grayscale information, segmenting the darkest parts of the annual lines. This segmentation will not reveal the exact borders between the lines, but only roughly approximate the positions. By using edge detection prior to segmentation, the line edges will be enhanced. Tracking by edges instead of grayscale information will reveal the exact borders between the lines. There will be no need to fit a parabola to the intensity profile since the intervals of the edge response is bounded by zero crossings.

The method of edge detection and enhancement used in this work originates from a fingerprint enhancement algorithm presented in the compendium by Danielsson et al. [3], where line detection involving the 2<sup>nd</sup> degree derivative of the fingerprint image is used to enhance the ridges of the fingerprint. Local line orientation not corresponding to the semi-global orientation is suppressed based on how much they deviate. This algorithm is implemented in the image processing program MIPS [4]. In [2], Sjöberg uses this FPE algorithm to enhance annual rings of a board cross section. This works well for annual rings, but requires more modification to work for annual lines since fingerprints patterns are more closely related to annual *rings* than annual *lines*. An opportunity arose to meet with PhD Maria Magnusson, one of the authors of [3], to discuss the FPE algorithm, this proved to be very valuable in the process of understanding and adapting it for annual lines.

Unlike, both [2] and [5], the algorithm presented in this report does not utilize binarization to segment the pattern. This algorithm preserves all intensity information throughout the whole process, the line tracing described in this report can for this reason, unlike the line tracing in [5], utilize information about both intensity and direction which makes it possible to locate the line borders with a precision of a single pixel.

## 2 Algorithm for detection of annual lines

The problem can be broken down in smaller problems; an overview is shown in Figure 10. To find the positions of the line borders, they must first be separated from the rest of the board, this is done with image segmentation. Since the borders of annual lines are characterized by a quick transition (step) from late wood to early wood, an edge detector based on the image gradient should give a strong response to these transitions.

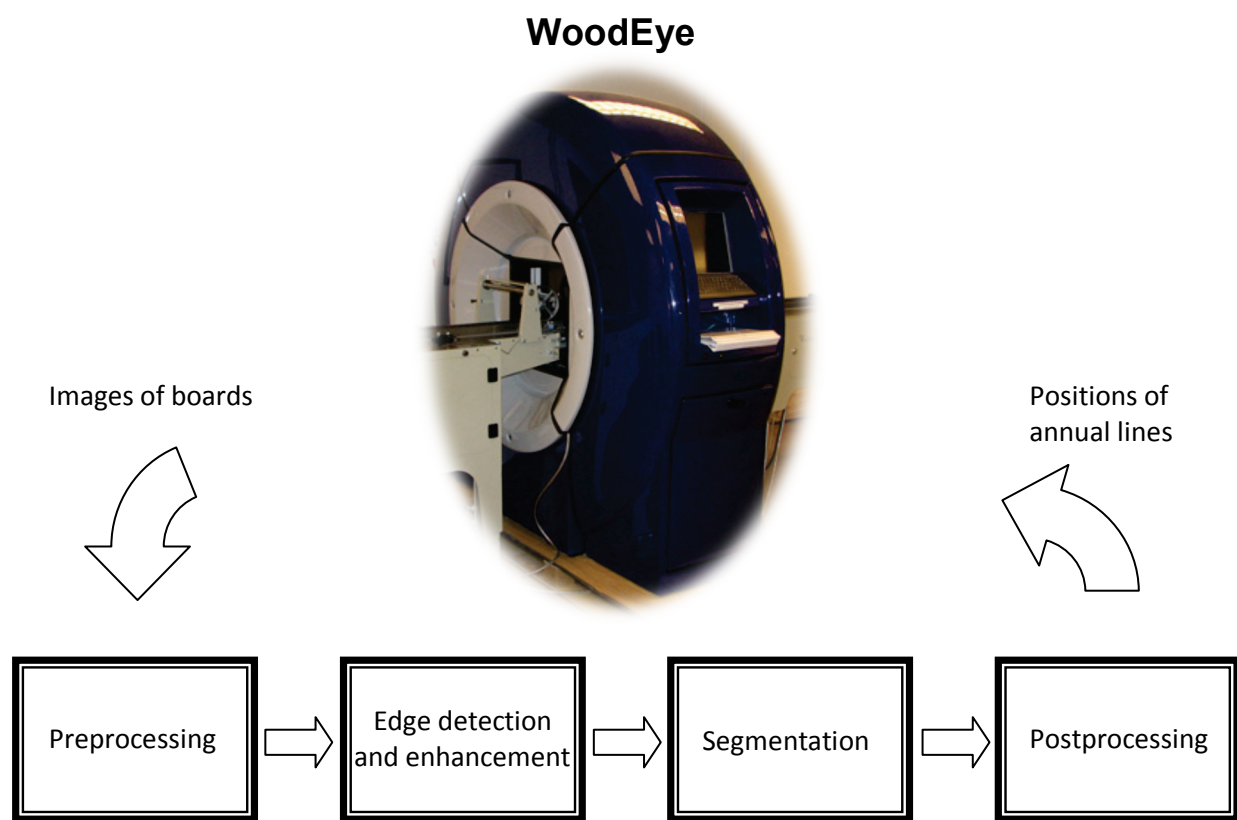


Figure 10: A high level overview of the ALD algorithm.

To improve the result of the edge detection, some preprocessing steps are made. Adaptive histogram equalization is applied to the part of the image that is to be processed; this does not only increase the contrast but also normalizes the image brightness in case of inconsistent lighting. It is also important to find the borders of the board in the image to remove redundant information like the background. Further, these borders will generate strong responses in the edge detection, by knowing their positions they can be excluded from the segmentation process.



## 2.1 Fingerprint enhancement

Based on the conclusions drawn in chapter 1.4.2, a fingerprint enhancement (FPE) algorithm was adapted for the purpose of enhancing annual line patterns. First, the adapted algorithm will be explained, and later the changes will be discussed.

The basic idea with the FPE algorithm is to compare local pixel orientation with the overall orientation within a larger, semi-global area. The semi-global orientation is generated by low-pass filtering the edge response, suppressing local variation and only showing the slower underlying variations. If the local orientation of a pixel doesn't correspond to the semi-global orientation, the pixel is suppressed depending on the amount of angular deviation. This way, high frequency variations like noise that does not follow the general direction will be suppressed.

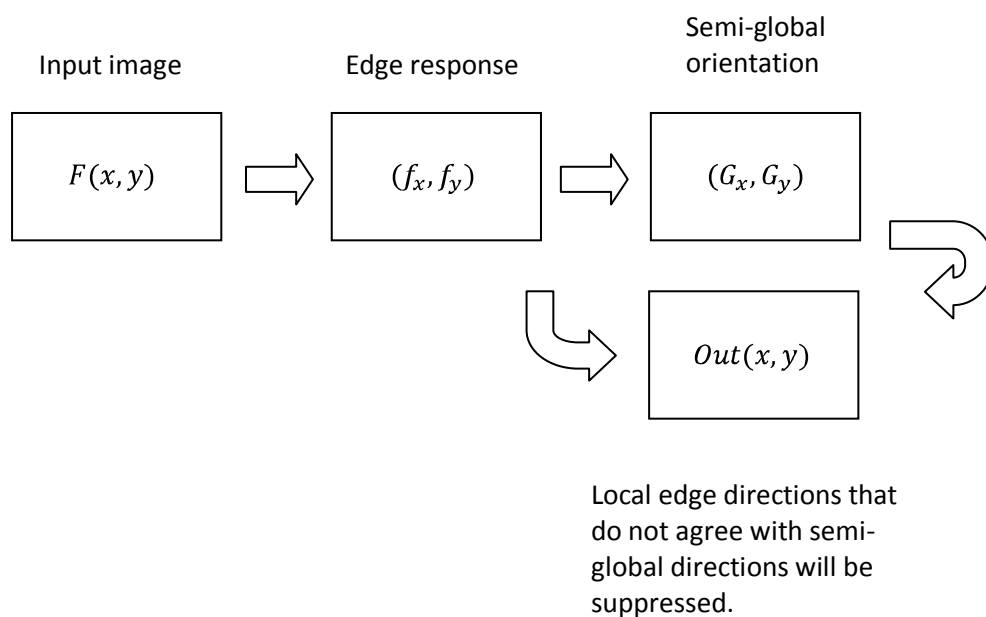


Figure 11: The FPE algorithm

### 2.1.1 Edge detection and enhancement

A common method for detecting discontinuities in grayscale images is edge detection by digital differentiation. By differentiating the image with respect to  $x$  and then  $y$ , the gradient can be formed.

$$\nabla f = \begin{bmatrix} f_x \\ f_y \end{bmatrix} = \begin{bmatrix} \frac{\partial f}{\partial x} \\ \frac{\partial f}{\partial y} \end{bmatrix}$$

Important information when dealing with the gradient is its magnitude

$$|\nabla f| = [f_x^2 + f_y^2]^{1/2} = \left[ \left( \frac{\partial f}{\partial x} \right)^2 + \left( \frac{\partial f}{\partial y} \right)^2 \right]^{1/2}$$

And the gradient direction

$$\beta = \arg(f_x + if_y)$$

The gradient method detects the edges by looking for local maxima and minima in the first derivative of the image. The digital equivalent of  $f_x$  and  $f_y$  is created by convolving the image with a differentiating filter. There are several variations of these filters and the one used in this report is the sobel filter.

1	0	-1
2	0	-2
1	0	-1

1	2	1
0	0	0
-1	-2	-1

Figure 12: The Sobel operators.

The sobel operator pair is not completely rotational invariant, but this is not a major concern since the main direction of the line-pattern is known, and does not vary much. This is one of the simplifying differences between fingerprints and annual rings brought up in conclusion 2. The pair can handle all the angles any line-pattern will appear in as long as the

main direction is known, which is always along the long side of the board. More about this in chapter 3.1.

### 2.1.2 Semi-global orientation

The normal to an edge can be described as a vector composed of the x and y derivatives of the edge and runs perpendicular to the direction of the edge. The angle of the gradient direction can be described as:

$$\beta = \arg (f_x + if_y)$$

A dark-light edge will have a positive derivative and a light-dark edge will have a negative derivative. Since the intensity in the gradient rises and falls as it describes the lines in the line-pattern, an intensity profile will show a negative inverse peak for every positive peak. This means that every other edge will have the opposite orientation even if the annual lines are running in the same direction (see Figure 14). It is impossible to generate a semi-global orientation through low-pass filtering if the pattern looks like this since the negative signals will cancel out the positive signals.

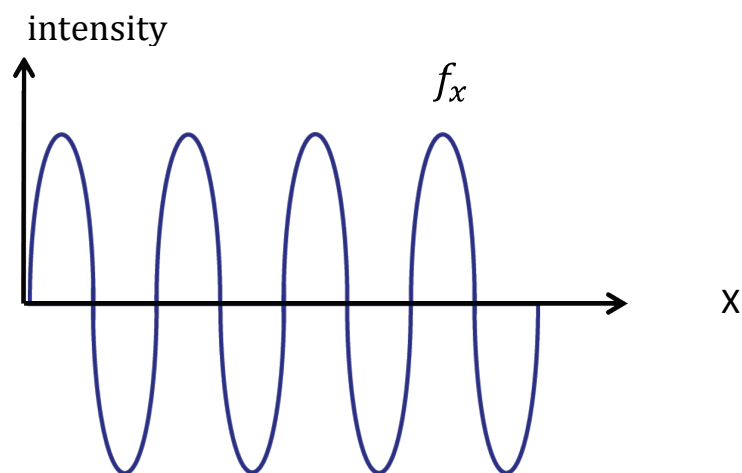


Figure 13: The intensity of the gradient rises and falls as it describes the lines.

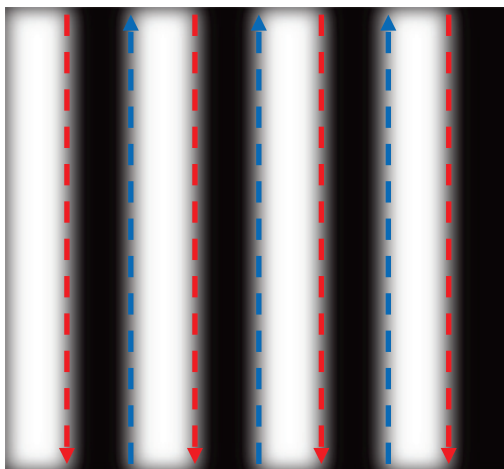


Figure 14: Direction of edges.

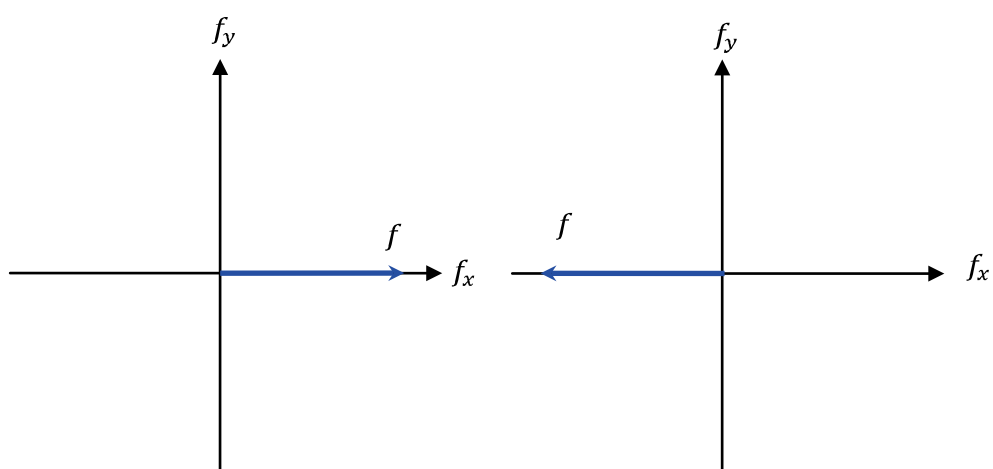


Figure 15: When  $f_x$  change from positive to negative, the gradient vector  $f$  will point in the opposite direction

### 2.1.3 Double angle

A solution to the problem described in chapter 2.1.2 is to use the double angle representation. This method is described in [2] and [3] and it can be tested using the image processing program MIPS [4].

An object looks the same after a rotation of  $360^\circ$ , but a line will look the same after a rotation of only  $180^\circ$ . This causes problems for consequently describing the direction of edges. To be able to find the average gradient direction in a larger area, the directions of edges need a uniform representation. This is possible by using the double angle representation. By doubling the angle of the gradient vector, any angle  $\beta$  and its counterpart  $\beta + \pi$  will equal  $2\beta$ . See Figure 16, and equation 1 and 2.

$$\beta * 2 = 2\beta \quad (\text{eq. 1})$$

$$(\beta + \pi) * 2 = 2\beta + 2\pi = 2\beta \quad (\text{eq. 2})$$

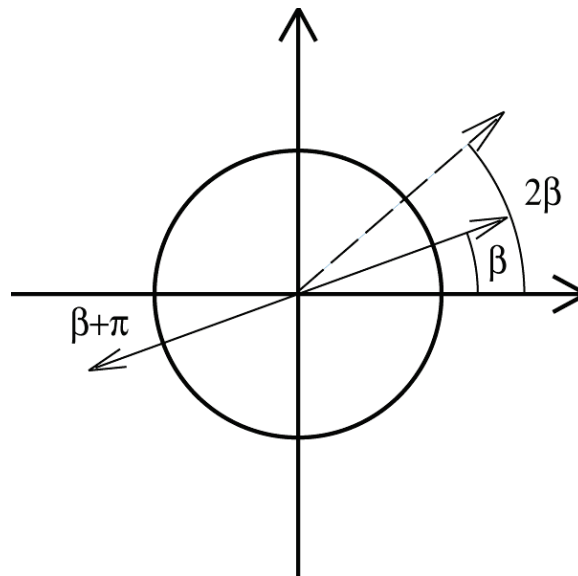


Figure 16: The effect of doubling the directional angles of a line.

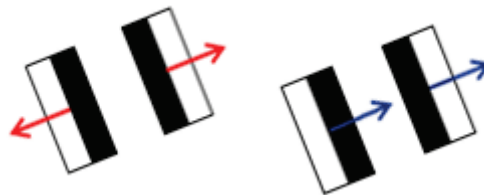


Figure 17: After doubling the angle, a light-dark edge will have the same direction as a dark-light edge.

The transition from single to double angle is achieved through a change of basis, where the vector  $f$  is rotated to double its angle. The length of the vector is preserved during the rotation.

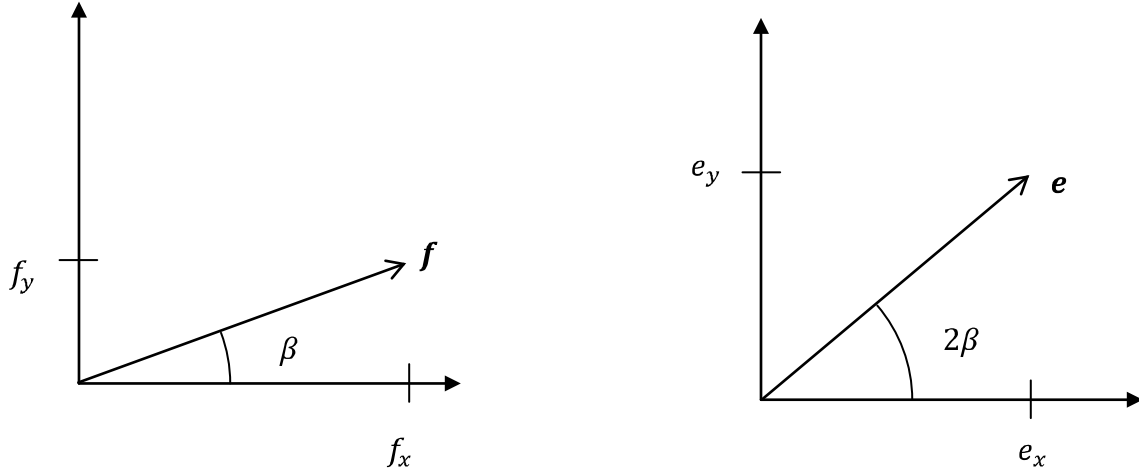


Figure 18(a): An edge described as a vector of its derivatives  $f_x$  and  $f_y$ .

(b): The edge in double angle representation.

$$f = \begin{bmatrix} f_x \\ f_y \end{bmatrix} = \begin{bmatrix} |f| \cos \beta \\ |f| \sin \beta \end{bmatrix} = \begin{bmatrix} \sqrt{f_x^2 + f_y^2} \cos \beta \\ \sqrt{f_x^2 + f_y^2} \sin \beta \end{bmatrix}$$

The length of vector  $f$  is preserved during the rotation from  $\beta$  to  $2\beta$ ,  $|f| = |e|$

$$e = \begin{bmatrix} e_x \\ e_y \end{bmatrix} = \begin{bmatrix} |e| \cos 2\beta \\ |e| \sin 2\beta \end{bmatrix} = \begin{bmatrix} |f| \cos 2\beta \\ |f| \sin 2\beta \end{bmatrix} = \begin{bmatrix} |f| \cos^2 \beta - |f| \sin^2 \beta \\ |f| 2 \sin \beta \cos \beta \end{bmatrix}$$

$$e_x = |f| \cos^2 \beta - |f| \sin^2 \beta = |f|^2 \cos^2 \beta - |f|^2 \sin^2 \beta / |f| = \frac{f_x^2 - f_y^2}{\sqrt{f_x^2 + f_y^2}}$$

$$e_y = |f| 2 \sin \beta \cos \beta = 2|f| \sin \beta |f| \cos \beta / |f| = 2f_x f_y / \sqrt{f_x^2 + f_y^2}$$

$$e = \begin{bmatrix} e_x \\ e_y \end{bmatrix} = \begin{bmatrix} f_x^2 - f_y^2 / \sqrt{f_x^2 + f_y^2} \\ 2f_x f_y / \sqrt{f_x^2 + f_y^2} \end{bmatrix}$$

When all edges are represented uniformly, the  $e_x$  component will look like in Figure 19. Figure 13 shows the same signal before the change of basis. This signal can now successfully be low-pass filtered to form the average value over an area. When the image is low-pass filtered, or smoothed, each pixel value will be the average value of a neighborhood centered over the pixel.

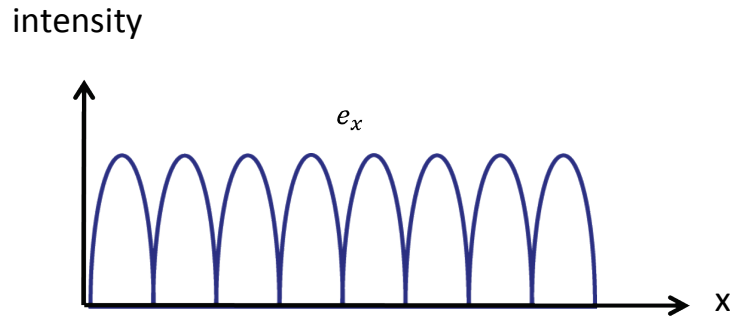


Figure 19: A 1D description of the derivative in double angle representation.

The local orientation of edges  $(f_x, f_y)$  are compared with the dominant, semi-global orientation  $(E_x, E_y)$  to find and suppress deviations. The angular deviation determines how much the signal will be suppressed by forming the scalar product between  $(f_x, f_y)$  and  $(E_x, E_y)$ .

### 2.1.4 Modifications

This method of edge detection originates from the FPE algorithm described in [2] and [3]. Some modification has been made which of the most important are;

- Edge detection instead of line detection
- Removal of the initial low-pass filtering

An edge detector based on the 1<sup>st</sup> order derivative was used instead of the 2<sup>nd</sup> order derivative line detector used originally. A 1<sup>st</sup> order detector has a stronger response to steps than a 2<sup>nd</sup> order detector as explained in Digital Image Processing [1], and it is also less sensitive to noise.

Another important change is the removal of the initial low-pass filtering of the input image. This filtering is meant to attenuate frequencies higher than the frequency of the ridges in the fingerprint. The cut-off frequency is set by adjusting the number of times the image is filtered. But because of conclusion 1(b), and that the process need to be fully automated without any manual parameter adjustments between boards, the low-pass filtering was removed completely from the process. The trade-off to eliminating the risk of losing information due to a faulty estimated cut-off frequency is that no high frequency noise, cracks and shade variations are filtered out at this stage.

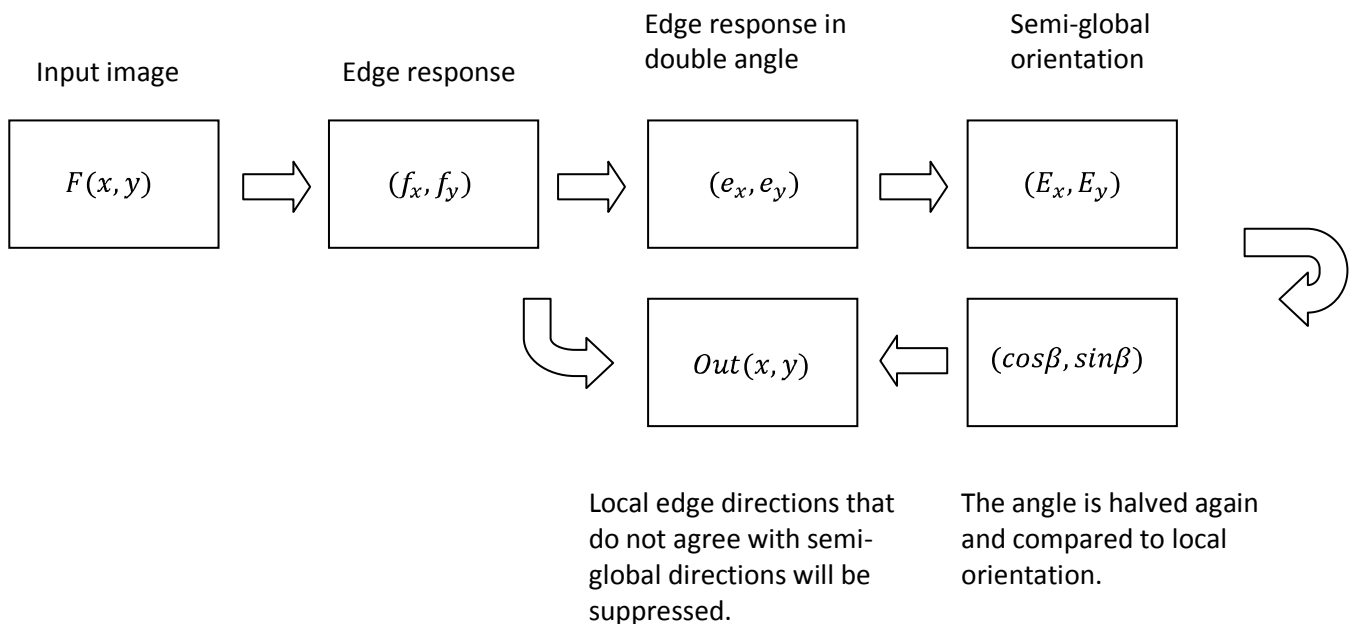


Figure 20: The final FPE algorithm



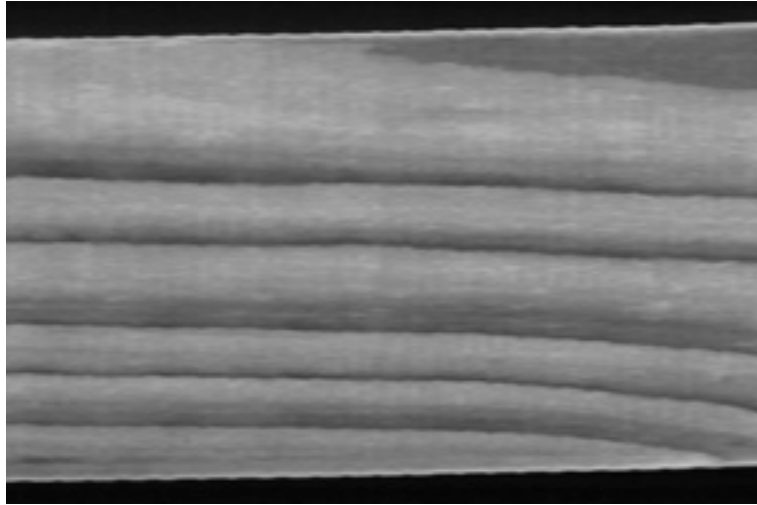


Figure 21: An image of a board section, before it has been processed by the FPE algorithm.

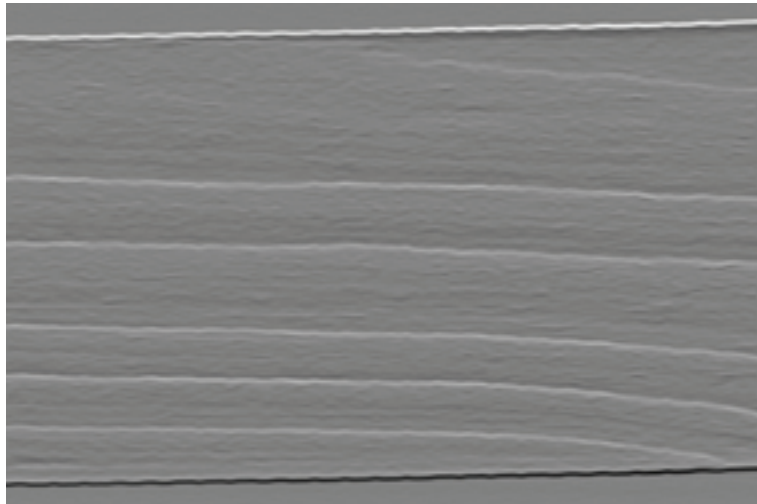


Figure 22: The same board section, after being processed by the FPE algorithm. Note the different intensities of the board edges.

## 2.2 Determining the growth direction and finding the seed points

The method of segmentation used is an algorithm called linetrace. It is a region growing algorithm that starts from seed points at a single column of the out-image, and grows them into one pixel wide lines while tracing the line edges.

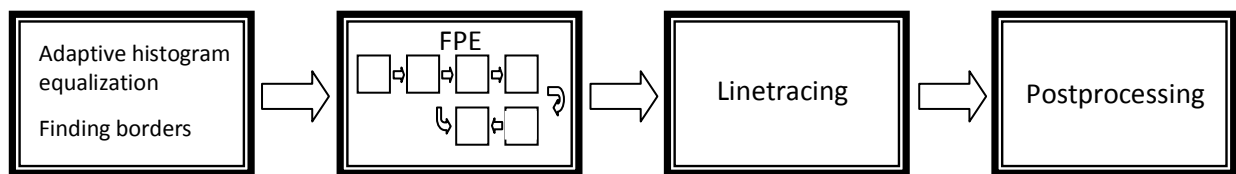


Figure 23: The ALD algorithm.

The out-image is a derivative of the board section which means that the strongest responses in the image is generated by the line borders. Every annual line will generate two signal responses, a stronger response caused by the quick transition from late wood to early wood (L-E), and a generally weaker response generated by the gradual change from early wood to late wood (E-L), see Figure 26. The signals has the opposite signs since the change in intensity goes from high to low for the E-L edge and low to high for the L-E edge . The L-E responses are usually sharper and more distinctive than the E-L responses, the peaks of these responses marks the borders between annual lines. It is not always the case that L-E responses are stronger than E-L responses, it is often very hard to make this distinction for thin lines. This can be seen to the right in Figure 26.



Figure 24: Here, the L-E transitions are a lot more distinct than the E-L transitions.

A transition of low intensity to high intensity generates a positive derivative. If the growth direction on the surface goes from left to right, the L-E transitions will generate positive peaks. If the direction goes from right to left, the L-E transitions will generate negative peaks (See chapter 1.4.4). It is therefore very important to find out the growth direction to determine which signals represent the line borders.

The E-L response is not a signal we are interested in at this point since it is not the border between annual lines, but these signals are discussed in the end of this report as an extension of this method with the purpose to find the ratio of late wood in the board.

Figure 25 describes the intensity profile of the board. The big step in the beginning and the end of the image is the responses to the edges of the board. The intensity fall at  $x = 90$  is a crack in the board. Otherwise, the annual lines seem pretty clear to make out with the bare eye.

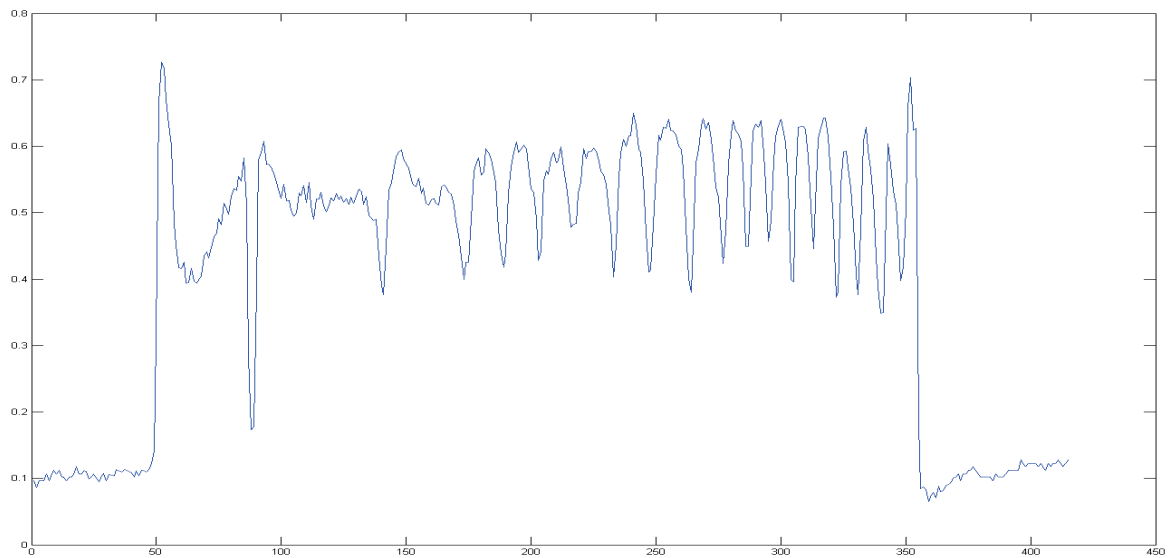


Figure 25: An intensity profile.

The plot in Figure 26 is the same profile but after the image has passed through the FPE algorithm. This shows the gradient instead of the grayscale. Here the peaks represent transitions from dark to light (increasing intensity), and the inverted negative peaks represent transitions from light to dark (decreasing intensity). Several methods was developed and tested to find the growth direction, and below is a presentation of the most promising.

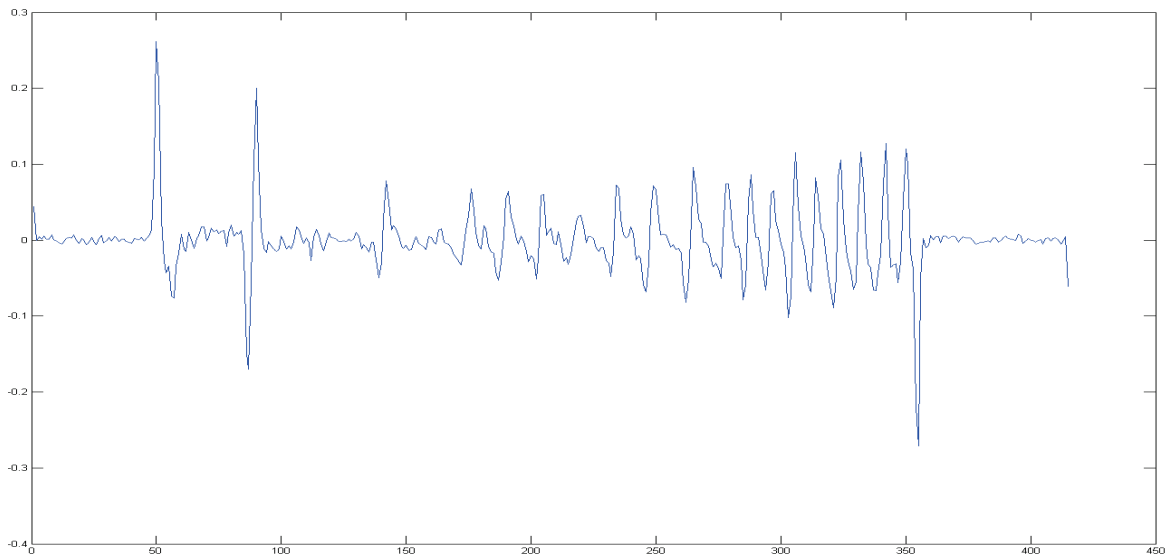


Figure 26: The gradient profile.

### *Derivative pixel count*

The idea of this method is to find if the low-high or the high-low intensity transitions in the gradient profile are the fastest. If the growth direction is from left to right, the low-high transitions will be the fastest. These transitions have a positive slope and will generate positive peaks in the gradient profile. If the growth direction is from right to left, the high-low transitions will be the fastest. A high to low transition is a negative slope and will generate negative peaks in the gradient. A steep slope contains fewer pixels than a gradual slope, this means that if the positive peaks are steeper than the negative peaks, the number of positive pixels in the gradient will be less than the number of negative pixels. The intensity of the responses does not matter since the number of pixels and not the value of them is compared.

### *Line width approximation*

This is a post processing directional finder. It is used together with any of the post processing estimation methods after the line borders have been detected to find out if the early estimation was right. Annual lines are generally thicker near the pith, with local variations occurring. But looking at annual lines over the whole width of the board, the direction of growth can be determined by comparing the annual line widths. This method utilizes the already segmented line borders to find the growth direction. If the preprocess estimation is wrong, the traced paths may be distorted and some may even be missing, but during testing the line distance approximation method provided 100% correct estimations

over 36 samples on 10 different boards, whereof 6 faulty preprocess estimations was properly corrected.

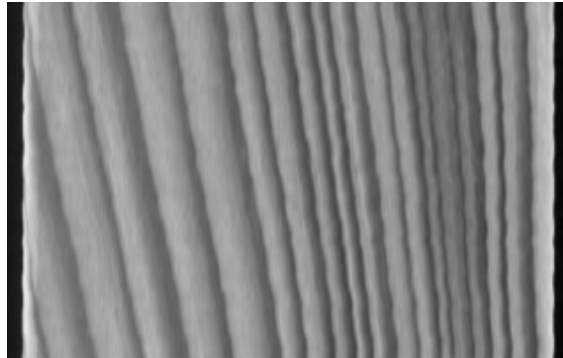


Figure 27: The annual lines to the left are wider than those to the right. This means that the pith is located somewhere to the left of the board, and the growth direction is from left to right.

### *Curve fitting*

A first or second degree polynomial is fitted to the absolute value of the gradient profile in a least square sense. By fitting a straight line, the line edge density can be estimated over the board. The slope determines which side of the board the pith is located; a positive slope places the pith to the left, and a negative, to the right. Fitting a second degree polynomial was looked in to as a way to find the pith if the pith was located within the board. This method need more work before it can be implemented into this algorithm.

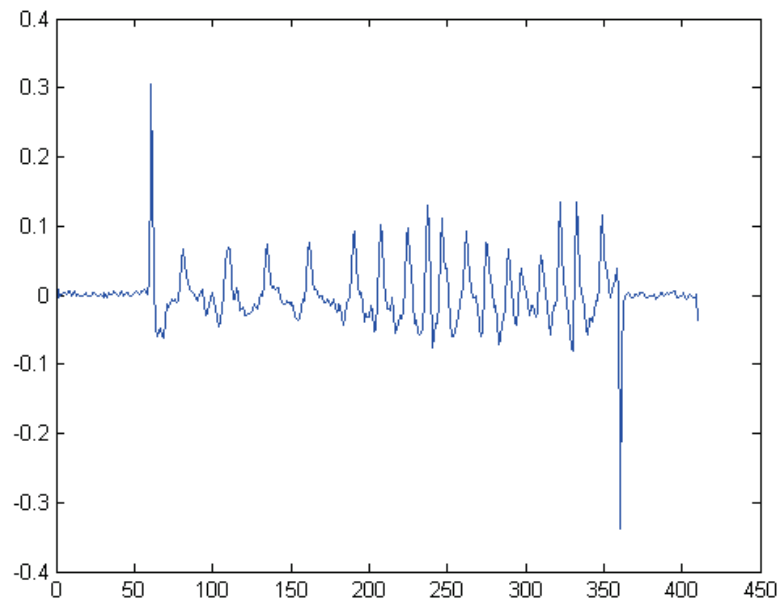


Figure 28: A gradient profile of the board in Figure 27.

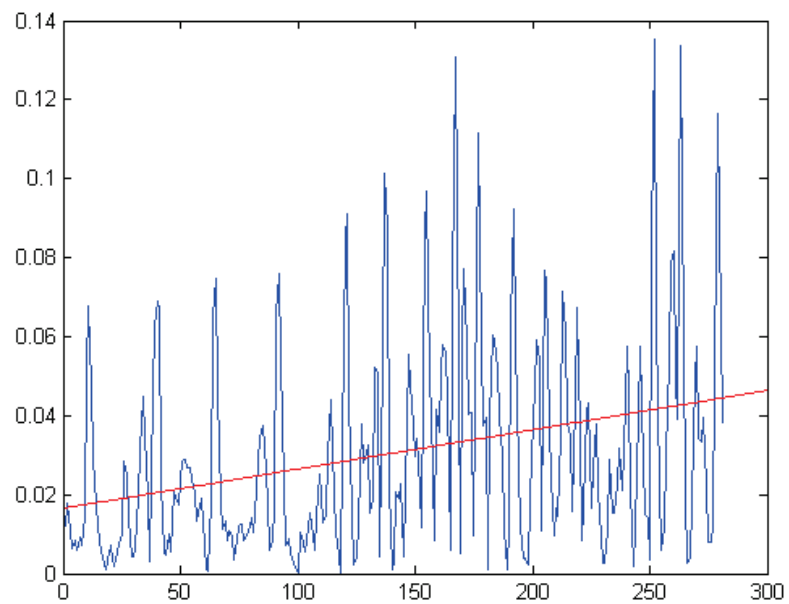


Figure 29: A line is fitted to the absolute value of the gradient profile after redundant information has been removed. The slope of the curve shows that the pith is located somewhere to the left of this board.

When a reversed direction of growth is detected, the gradient image is inverted (multiplied with -1) to change the sign of the peaks to make them positive. This is done so the linetrace algorithm can trace by local *maxima* regardless of direction of growth.

By determining whether the positive or the negative local extremes are the borders, roughly half of the peaks are ruled out. All the peaks with the right sign are used as seed points in the linetrace algorithm.

It becomes more complicated when the pith is located within the board. Since the wood is growing radially outwards from the pith, the board may include annual lines that have been growing in opposite directions as seen in Figure 31. This means that on one side of the pith, positive peaks represent the borders, and on the other side of the pith the borders return negative peaks.

The solution to this is to first run linetrace normally, then invert the out-image to trace by the negative peaks, and run a second trace above the topmost found line, or below the lowest found line - depending on the growth direction.

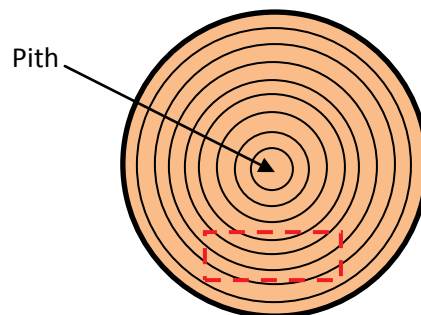


Figure 30: The location of the pith.

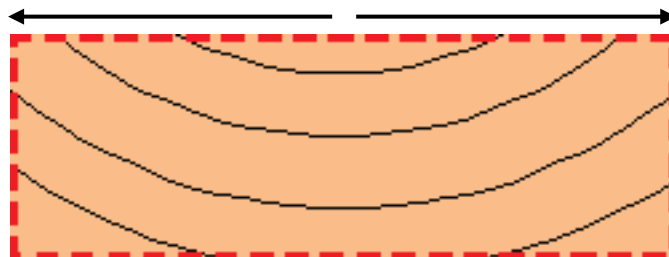


Figure 31: The lines on the up and down side of the board has grown in opposite directions.

## 2.3 Linetracing

Linetrace is a type of directional region growing algorithm. The basic idea is to create a one pixel wide path along the annual line borders by tracing along the maximum intensity pixels in the out-image. The pixel-path is, if completed, saved after the trace and a new trace is started from next seed point. The linetrace algorithm is quite tolerant to noise. All lines being traced are tested against multiple criteria both during and after the trace. A trace starting from a seed point that is not on a border edge will eventually;

- 1) Die out, since noise is not continuous in the same way that lines are (conclusion 3).
- 2) Be cancelled by one of the rules.
- 3) Trace onto a border edge, since the trace process is constantly searching for local maxima.

By taking advantage of the knowledge that annual lines runs from one end of the board to the other, the trace kernel only need to look at the pixels in one direction, in this case, the three pixels to the right. In the most basic case the algorithm selects the pixel with the highest intensity value and adds it to the pixel-path. This simple kernel k-3, seen in Figure 32(a), is fast and provides a good result on most line-patterns with the exception of the more curved patterns that occur near knots. Several types of kernels was tested, a slightly more complex kernel k-5, shown in Figure 32(b), was developed to counter a tracing error where k-3 lost track of the border edge due to sharp one-pixel wide noise. K-5 looked at a wider path by weighing in the neighbor pixels *D* and *E* and could ignore the noise and keep on track. Lastly from testing, kernel k-8 evolved, Figure 32(c). This trace kernel looks one step ahead to decide which way to go. For example, when weighing the sum for pixel *A*, it adds the maximum of *D*, *E* and *F* which is the next triple to choose from if *A* is chosen. The weights for *B* and *C* are calculated in the same way, which leads to the result that pixel *F* can be discarded from the sums since it is present in all three equations and will not affect the outcome.

Even though the kernels look at different neighborhoods, they all chose between pixels *A*, *B* and *C* to decide which pixel to add to the pixel-path. The only difference is the information the decisions are based upon.

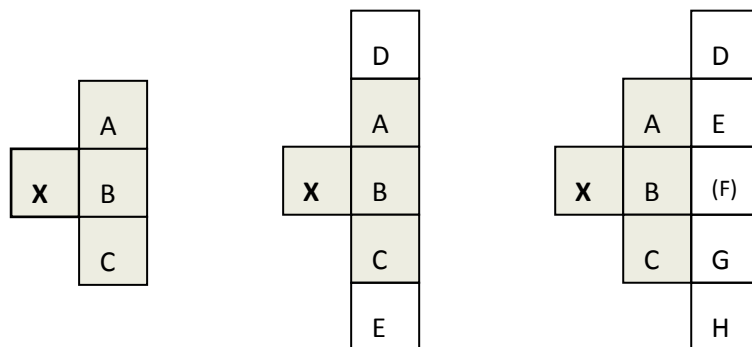


Figure 32(a) : k-3

(b) : k-5

(c) : k-8



Some validity checks are made during the linetrace procedure, if any of these checks trigger a warning the program will respond with an attempt to correct the line depending on the type of warning.

### *Vertical correction*

For every trace, a mean intensity value is kept over a semi-global history of pixels in the traced pixel-path. For every iteration, this value is compared to a local mean over a more recent and shorter history. If the ratio of the local to the semi-global history mean falls below a threshold, an intensity deviation warning is issued. The trace may have lost track of the border edge and may be randomly floating.

The basis for this correction is the priori knowledge in conclusion 1(a). Firstly, a control is made that the path has kept a fairly constant distance to its neighbor (the last completed pixel-path). If it has, then a new position is guessed based on the distance it kept just before it lost track of the line edge. A search vector in the form of a column vector is applied to look for the most probable line pixel near the guessed position. The size of the column vector depends on the distance between the neighboring lines. It has to be large enough to find the right position even if the guessed position is somewhat displaced from the line, but not too large that it may accidentally select a pixel from any of the neighboring lines.

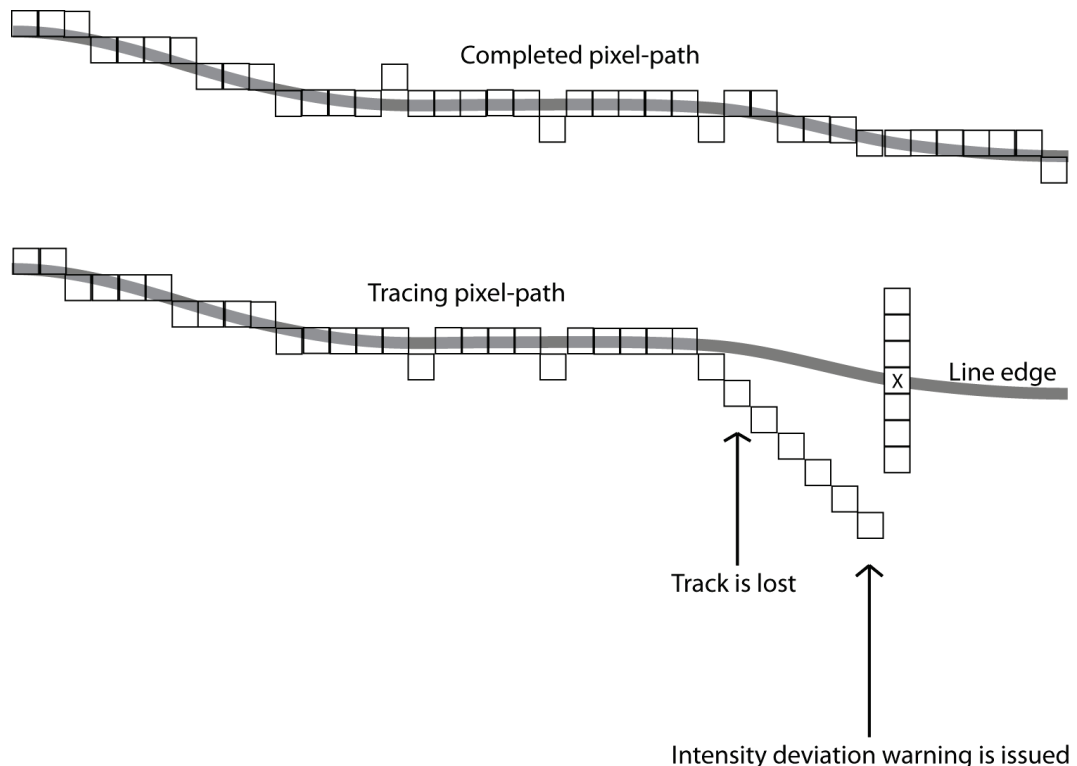


Figure 33: Vertical correction.

### Horizontal correction

If the trace is stopped because the values of the 3 available pixels are below 0, a special correction is used. Since no intensity deviation warning has been issued, there is reason to believe that the trace kernel is still on the border edge, but noise or other disturbances have rendered a limited segment of it unreadable. This problem needs a slightly modified correction since the border edge has been disrupted but will be traceable again beyond the disruption. The horizontal correction sends the search vector a number of pixels forward in the horizontal direction, trying to jump the gap in the border edge. The position is guessed the same way as in the vertical correction. Both the vertical and horizontal correction may cause a break in the pixel-path. This is repaired with interpolation between the end positions of the break.

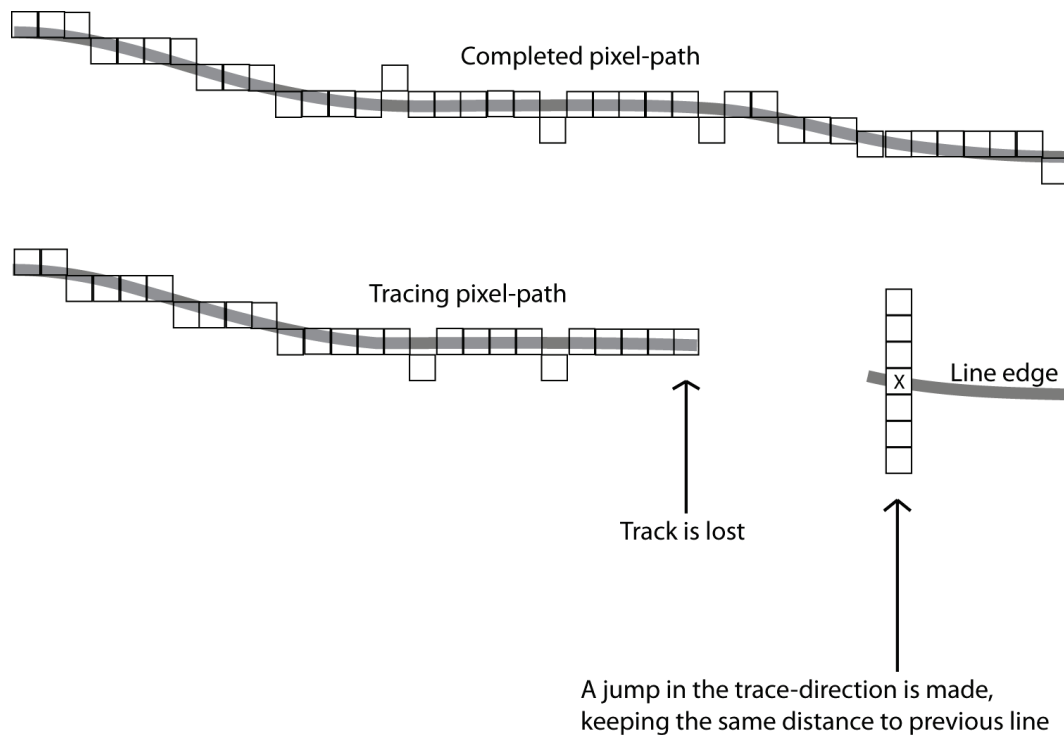


Figure 34: Horizontal correction.

The paths go through various other tests before being saved to the line-buffer. Some of these test for

- 35

### 2.3.1 Linetracing vs. Binarization

Many methods of fingerprint analysis use binarization to segment the ridges from the valleys, this method of segmentation is common in the field of annual ring analysis as well.

Binarization and morphology was considered for the next step in this report but was later dropped in favor of the Linetracing method described in 2.3. One of the most important reasons is that the image contains a lot of noise since the low-pass filtering was removed from the edge detection and enhancement process.

The out-image from the FPE algorithm can be binarized with an appropriate threshold and filtered a number of times with some suitable morphological operators like in [2]. But since annual ring width and contrast differ greatly from one board to another and even within the same board this approach needs extra input information or supervision during the process. Multiple thresholds would be necessary within the same image, and the morphology would have to be adapted depending on the width and signal strength of the borders. It is easy to try different settings until a good result is returned for an individual board, but harder when everything is automated. In addition, a thresholding operation will generalize all the pixels with a value above the threshold, discarding all grayscale information. By avoiding thresholding and keeping all the grayscale information in the out-image, the exact positions of the annual line borders can be located.

To find the edges through binarization and morphology, steps like thresholding, thinning, dilation, skeletonizing and line repair has to be iterated over the image. The linetrace algorithm presented in 2.3 performs every step in one iteration; from finding the lines, thinning them to one pixel wide and repairing broken lines. Also, by using priori knowledge about the character of annual lines (see chapter 1.4.2), linetrace will only run where it suspects a line may be located, hence it will operate only on a fragment of the image. Linetrace runs over the image once and it can handle annual rings with different character without manual change of parameters.

## 2.4 Validation of lines

After the segmentation process, the paths are validated for intensity and parallelity. Paths with weak mean signal strength are removed. Paths that does not run parallel to its neighbors are removed as well.

### 2.4.1 Piecewise segmentation

Since a linetrace starts from seed points determined at a given pixel column, lines introduced from the board edges will not be found by the trace procedure. This is solved by restarting the trace with new seed points from a column further along in the trace direction. This creates separate segments of traced pixel paths, and the idea is to introduce new lines coming in from the edge of the board, but also to validate the paths by connecting them piecewise through all of the segments. A path that, from its starting point cannot be connected through all the segments to its right will be classed as noise and removed.

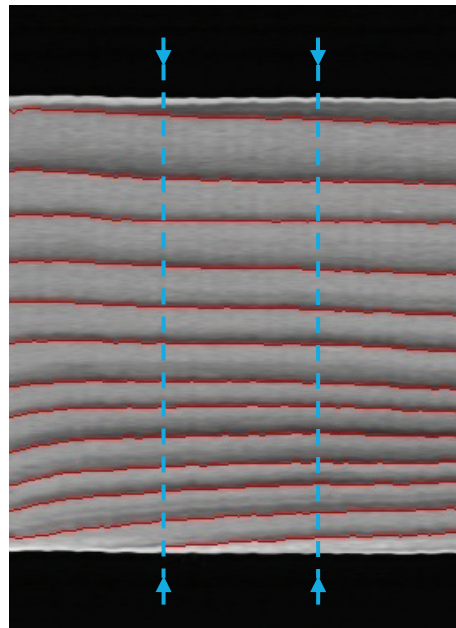


Figure 36: The first restart marked by the blue dotted line introduces a new line from the lower edge of the board.

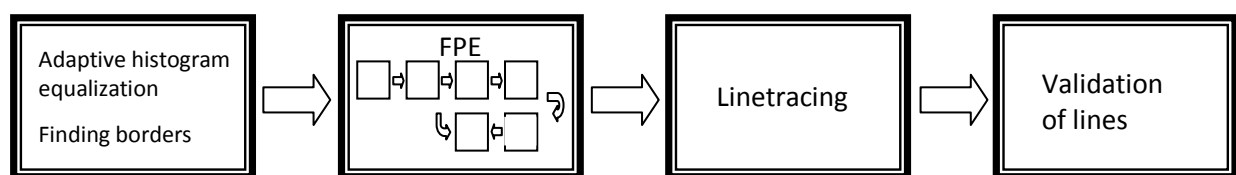


Figure 37: The final ALD algorithm.

### 3 Results

The method of piecewise segmentation described in chapter 2.4.1 can produce correctly segmented annual lines of virtually any length. Long segments are visually appealing when presented as a result of the segmentation, but goes beyond the purpose described in chapter 1.2.

The result required to satisfy the goal is to know the positions of annual lines on a one dimensional profile or column. The linetracing is performed to find and filter out the paths that do not pass as annual lines. The remaining start positions, or seed points, in that particular column match the positions of detected annual lines. As long as the annual lines can be positioned at the same longitudinal coordinate on all four sides, the goal is met. By using piecewise segmentation, annual line positions can be sampled from roughly any column within the processed board section.

Figure 38 - Figure 45 shows some results of the complete Annual line detection algorithm. These images are from the blue channel, they are scanned from the up and down sides of the boards. The image to the left shows the unprocessed image section and the image to right shows the result of the ALD algorithm superimposed on the board. Piecewise segmentation has not been used. Figure 40 shows an example where the algorithm failed to trace the annual rings due to the extremely high line density and low contrast. The lines in the lower part of the image are barely visible for the naked eye. In many images, false lines appear near the top and bottom of the board due to the strong edge response of the board edges. In an attempt to avoid these lines, a margin was introduced to prevent tracing too close to the board edges. Setting this margin to the right value is a delicate process, figure 41 and 42 shows the result of setting this margin too high, causing the trace to miss the annual lines near the lower edges. A solution to this problem is proposed in chapter 4.1.

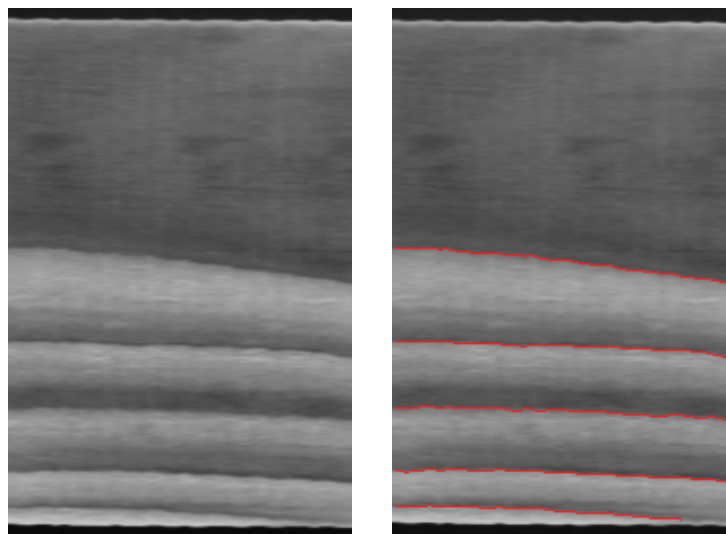


Figure 38: Test sample 1.

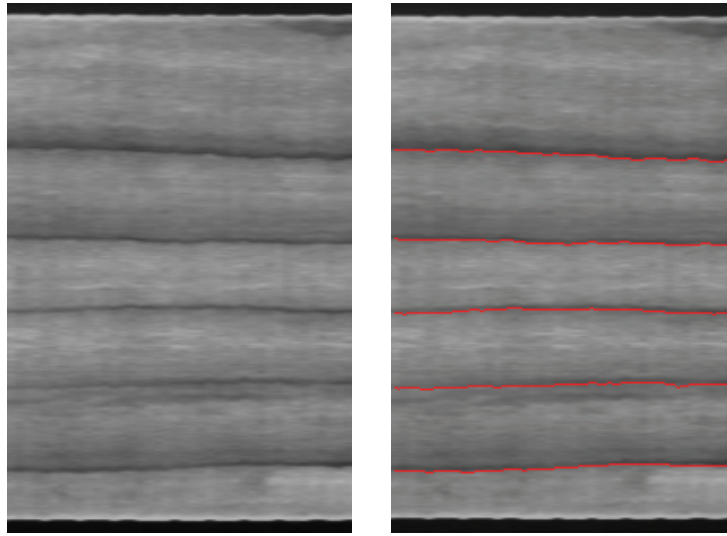


Figure 39: Test sample 2.

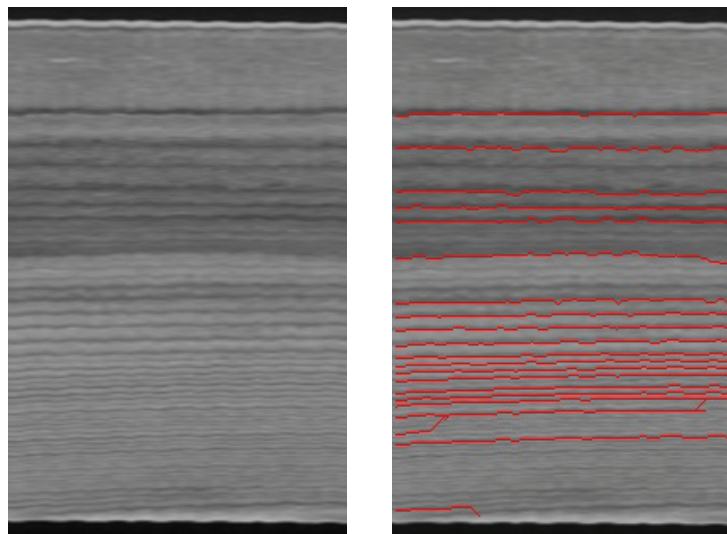


Figure 40: Test sample 3.

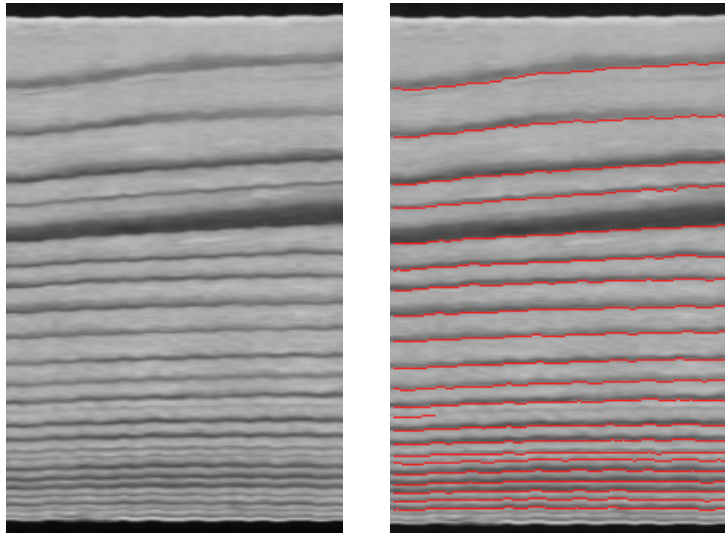


Figure 41: Test sample 4.

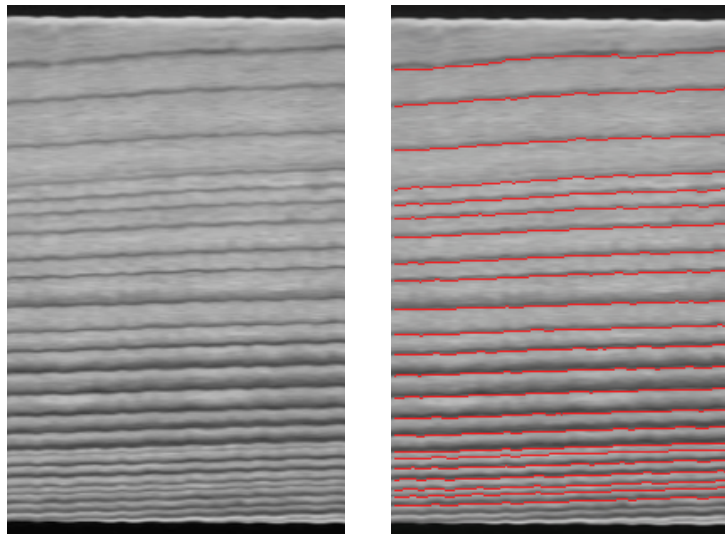


Figure 42: Test sample 5.



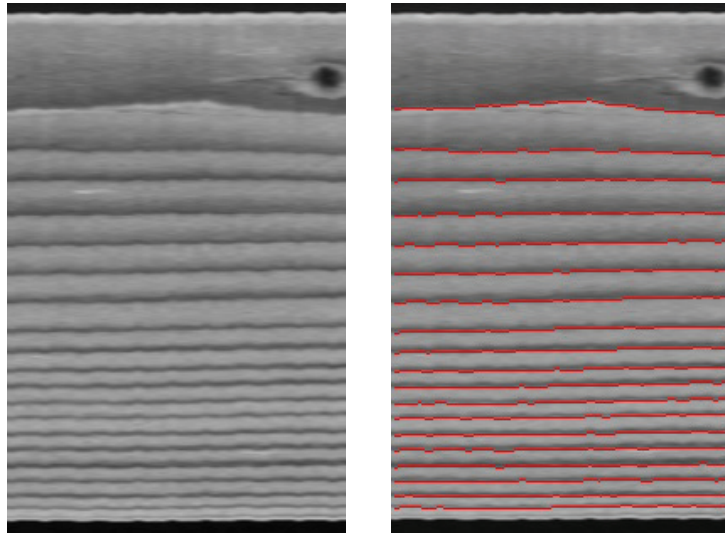


Figure 43: Test sample 6.

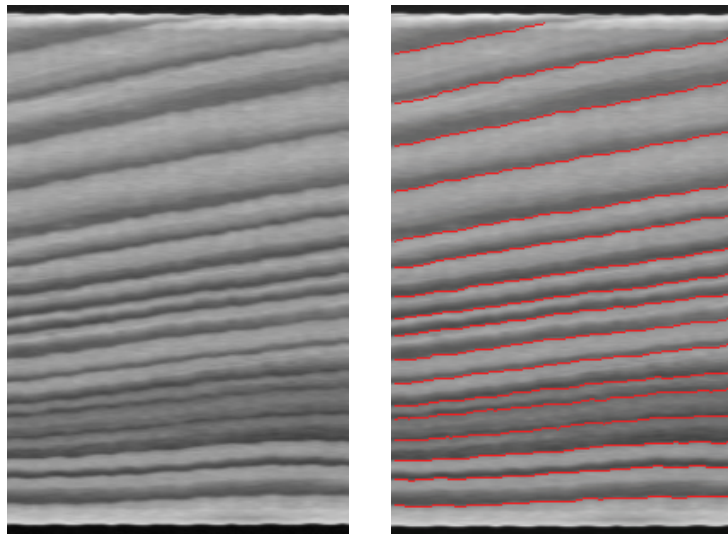


Figure 44: Test sample 7.

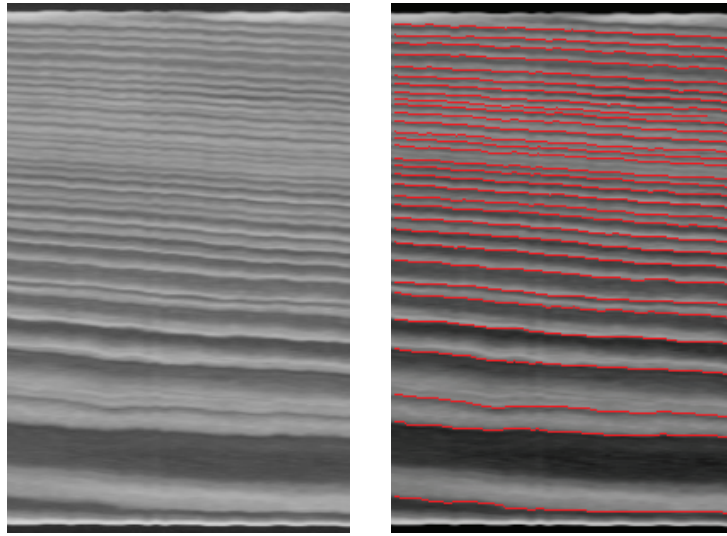


Figure 45: Test sample 8.

The RGB camera will only scan the up and down sides of boards. This means that images from the grayscale camera have to be used when the left and right sides of the boards are analyzed.

Figure 46 and Figure 47 show test images of annual line detection performed on all four sides of a board, starting from the same longitudinal position.

Figure 46: Line detection performed on all four sides of a board.

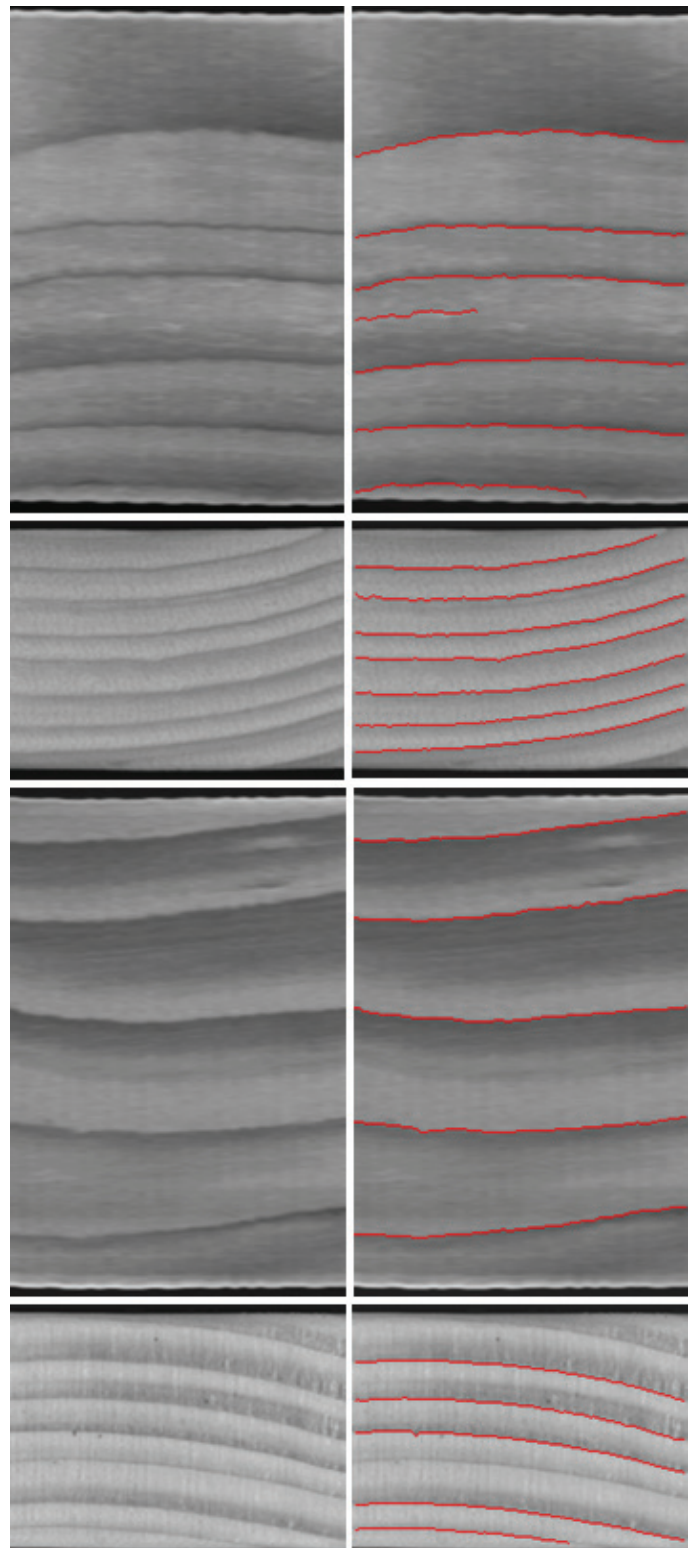
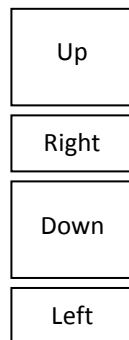
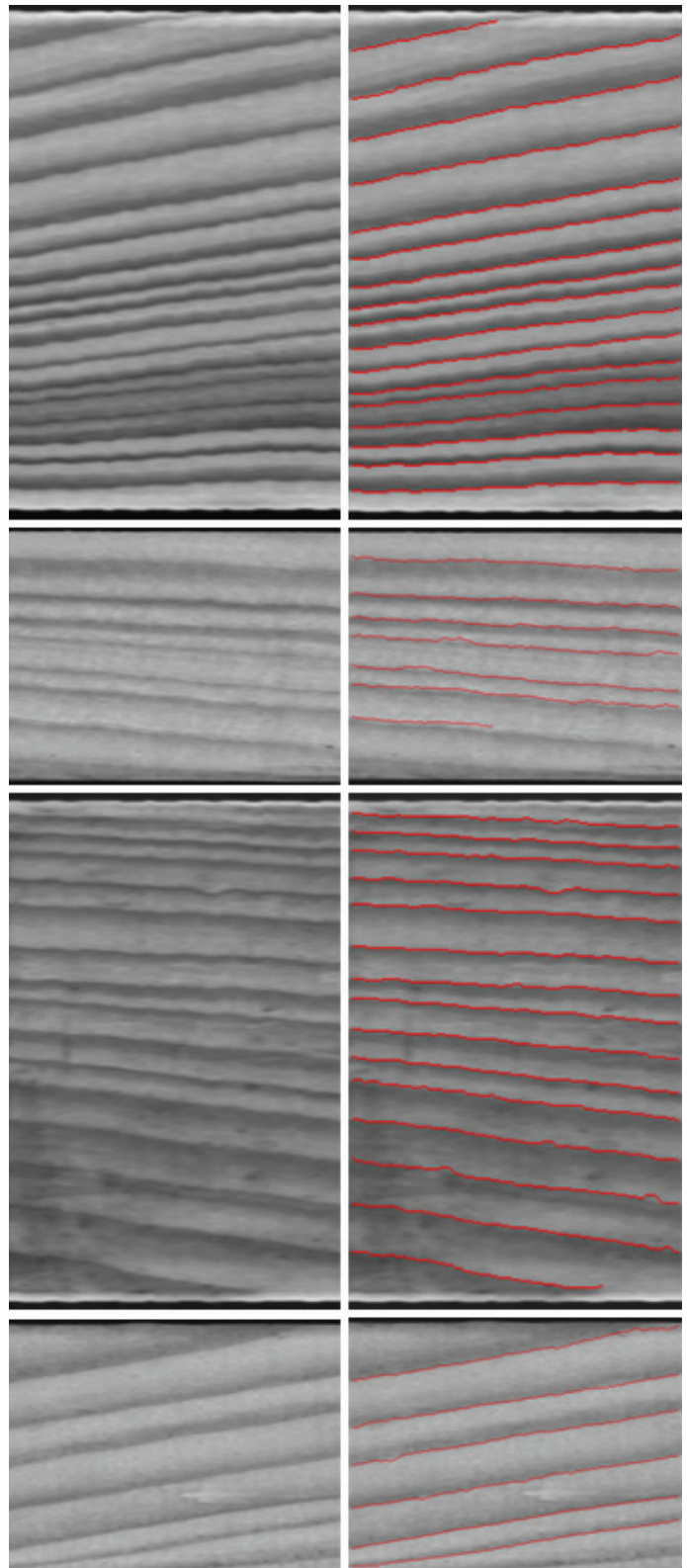
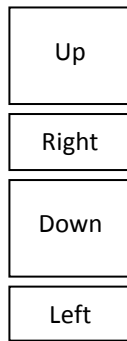


Figure 47: Line detection performed on all four sides of a board.



## 3.1 Discussion

### *Board sections*

The annual line detection algorithm can run on board sections of any length. For reasons explained in the definition of conclusion 3, the section should not be shorter than about 2.5 – 3.0 cm. The longer the section is the smaller is the chance that noise will pass as annual lines. But with a longer section, there is also a higher risk that any of the true lines are disrupted, and dropped.

The input image to the algorithm is preprocessed by WoodEye in order to provide the ALD algorithm with a defect-free board section. This is of great benefit since the character of the line pattern is disturbed near defects like knots and rot. Many of the conclusions drawn about line patterns in this report are made on the basis of a defect-free board section.

### *Sobel operators*

The sobel filter pair is not fully rotational invariant. A combination of these filters results in a gradual sign shift for edges at angles  $45^\circ$  and  $135^\circ$ . Through the change of basis described in chapter 2.1.3, the angle of this discontinuity is shifted to  $+90^\circ$  and  $-90^\circ$ . The cause of this discontinuity is that a doubling of angles  $\beta = 90^\circ$  or  $\beta = 270^\circ$  will create the new angle  $2\beta = 180^\circ$ , which is right on the limit of sign shift for the new  $e_y$  component (See Figure 16). This will cause a sporadic change of sign for small angular variations around these angles. Keeping conclusion 2 in mind, we know that annual lines have a distinct main direction, and that the angular deviations from this direction are small. By rotating the image of the board so that the main direction of the pattern is  $0^\circ$  or  $180^\circ$ , perpendicular to  $90^\circ$  and  $270^\circ$ , it is safe to assume that no lines will ever appear in the angles of discontinuity.

### *Contrast and noise*

The annual line detection algorithm can detect lines of boards with varying line density. But it encounters problems when line density is high at the same time as the contrast is very low, see Figure 40: Test sample 3. Further development in the preprocessing step to improve the contrast of the input images would benefit the whole algorithm. The same goes for reduction of noise. One area where better noise reduction could be implemented is in the search for seed points, where the gradient profile could be more thoroughly analyzed to reduce the number of seed points passed on to the linetrace algorithm. While this does not suppress noise in the image itself, it reduces the processing time by providing the linetrace algorithm with fewer start positions to trace from.

The validation phase is based on a set of validation rules, the settings of these rules is part of a delicate balance act to sort out the false lines caused by noise, and at the same time keeping the true lines. If these rules are unbalanced, false lines may appear in the result, or true lines may be dropped. Further increased contrast and reduced noise would increase the stability and robustness of this algorithm.

## 3.2 Tests

Several tests were made to compare the performance between different solutions. All the tests were made on defect-free board sections, since there is no reason to complicate the tests beyond what can be expected as input from WoodEye. The tests discussed here are enclosed in the appendix.

### *The trace kernel test*

This study compares the trace kernels k-3 and k-8 described in chapter 2.3. The test was done using the method of piecewise segmentation. It also includes a variation of the sobel filter operator size. The variable *sno* represents the number of times the operator is convolved with an averaging filter. The operator is a square with sides  $3 + 2 \times sno$ .

The test was performed on 8 samples from 3 different boards, with *sno* varying from 0 to 12, resulting in 51 different test images.

The result of this test shows that k-3 and k-8 performs exactly the same for defect free sections. K-8 will perform better when the line pattern becomes more complicated, like the increased curvings near knots. Because of the longer processing time of k-8 and that the input images will be defect-free, there is no reason to pick k-8 over the simpler k-3.

Adjusting the sobel operator size can be good for boards with wide annual lines. It can also be used for images collected from the grayscale camera because of the higher resolution compared to the RGB camera. A larger operator size will result in wider, but weaker edge responses. But the same problem arises as discussed in chapter 2.1.4, the initial low-pass filtering; without knowing the character of the lines in advance, it is risky to increase the size of the operator. As shown in the test, the slight advantage gained for boards with thick lines does not compensate for the damage that can be done to images of boards with thin lines. If a method of estimating the line density in a preprocessing step is developed, the sobel operator size and/or the cut-off frequency in the initial low-pass filtering can be set automatically.

### *The growth direction estimation test*

The growth direction estimation is a problem described in chapter 2.2. The problem gets more complicated when the pith is located within the board and lines with different growth directions are present. Several methods were developed and tried, which of one can detect if the pith is present in the board. However, this method was not further developed after testing, but could become a feature in the future.

Although a method of detecting the pith is not implemented, a solution to the problem of detecting lines with different growth directions exists. While it still needs adjustment, it is a solution with good prospects. The method consists of first running linetrace normally to find the lines with the growth direction initially estimated. Then the out-image is inverted to make linetrace trace lines with opposite direction. This second trace is run above the topmost found line, or below the lowest found line - depending on the growth direction.



In the example illustrated below, a top-down growth direction was detected. The linetrace algorithm found the lines that had been growing in this direction but not the line that had been growing upwards from the pith. The edge response was inverted and linetrace was iterated a second time, now tracing along negative peaks. This time, only the area above the topmost found line is traced since we are looking at the other side of potential pith. In this case the position of the pith is revealed indirectly, since a line is found in the second iteration.

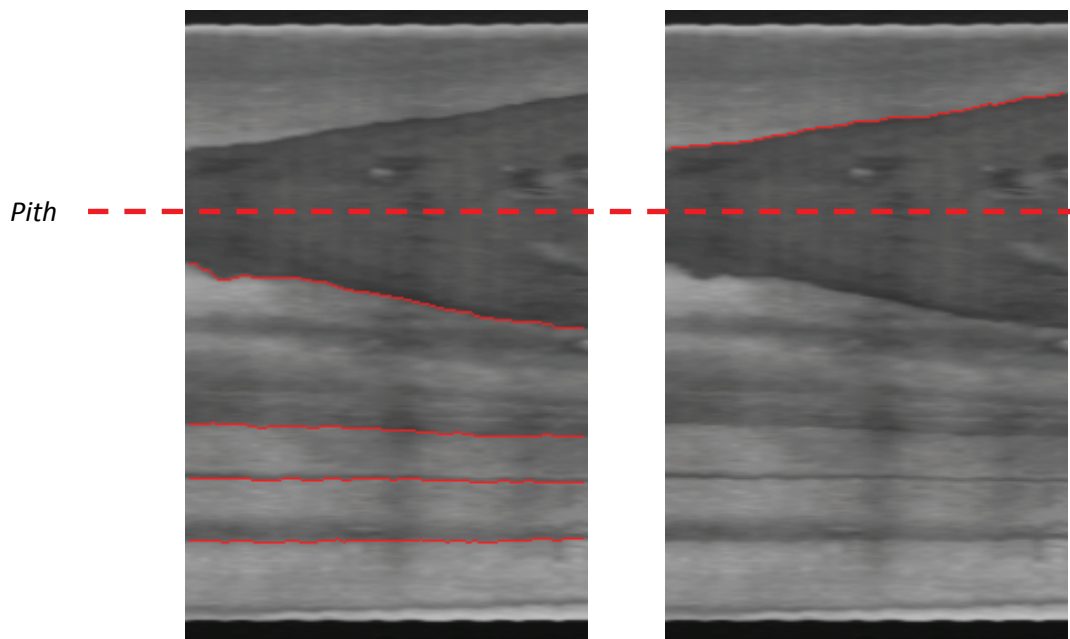


**Figure 47(a) and (b) :** The process of inverting the line response to find lines on the other side of the pith.

The growth direction estimation test shows that all methods of curve fitting outperform the Derivative pixel count method. The post processing method, Line width approximation should only be used as an indicator if the initial estimation is correct. Since it depends on the lines found after processing, an initially incorrect estimation or a bad segmentation could compromise the Line width approximation method. But as an indicator, if this method shows that the initial estimation is wrong, then something unexpected has likely happened. This can be a result of dropped or extra lines, or a faulty estimated growth direction.

### *The sensor comparison test*

The images used in the algorithm were collected from the grayscale camera and the blue channel of the RGB camera. Compared to the grayscale images, images from the blue channel have a higher contrast, but are of lower resolution. A test was performed to find out which one of these benefits was of more value to the algorithm. The test was done on 17 sampled sections of 5 different boards. Both grayscale and blue channel images were

resampled to equal size to be able to test the images under the same conditions regarding sobel operator size and other parameters.

The result of the test shows that the algorithm perform equally well with both image types on most boards, but the images from the blue channel sensor gives a distinctly better performance on boards with high line density and weak contrast. When the pattern is more difficult to analyze, images from the blue channel sensor is to prefer over images from the grayscale sensor. Blue channel images are, in the existing data set, available for the up and down sides of the boards. For the left and right side, grayscale images are used.

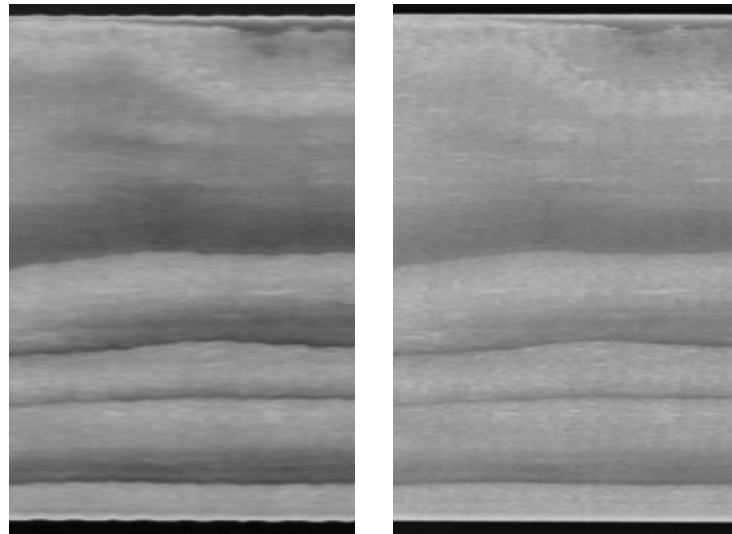


**Figure 48** (a): RGB blue channel. (b): Grayscale.



## 4 Conclusions

The purpose of this work was to develop an algorithm that detects annual lines on the surfaces of boards by using image processing. The algorithm should be fully automated and be able to analyze boards with little or no manual setting of parameters. The goal was to establish the positions of the annual lines on all four sides of a board, at a given longitudinal coordinate

The test results show that this goal has been reached for many types of boards with respect to the character of the line pattern. The exceptions are boards that have a high line-density at the same time as they have a very weak contrast. Once the optimum settings are found, the algorithm can handle most boards well.

Analyzing grayscale images will require different parameter settings than blue channel images will. In a hardware setup where RGB cameras are present, the up and down images from the blue channel are used, and the left and right images from the grayscale cameras are used. If there is no RGB camera present in the actual WoodEye configuration, images from the grayscale cameras are used. The only configuration information this algorithm needs to have is if WoodEye is using the RGB camera for up and down scans or not.

This algorithm is designed to be used for spruce. But as long as the annual lines are of fairly good contrast, and goes smoothly in the longitudinal direction, other types of wood may be successfully analyzed as well. Several tests have been done to optimize the performance of the algorithm, like the choice of trace kernel. However, methods and parameters can always be further optimized.

When creating the validation rules, a central thought was kept in my mind; how do the eye and mind interpret the cues to separate a true annual line from a line created by noise? And how do I translate these cues to code? Statistical analysis of pixel values, line smoothness and widths has also been used. The rules are based on a mix of cognition, and the more exact science of math.

Without the post processing validation rules, a lot of noise would be classed as lines. The conditional rules that are built into the linetrace algorithm set the line classing threshold quite low to avoid sorting out true lines. The most important validation takes place in the post processing, where methods detached from the bulk of the code takes care of the more delicate classing. This makes these rules and methods easy to modify, and new rules can easily be added to the validation chain.

It is important that this part of the algorithm is easy to update, even though the current rules works pretty well, they are quite basic and have only been tested on a limited dataset. But more importantly, these methods decide what will be sorted out, and what will be classed as lines and returned to WoodEye.

For future work, a good start would be to look over the preprocessing (contrast, noise) and the post processing (validation) steps, since these are easier to update and require less insight into the code of the algorithm.

## 4.1 Future improvements

While developing this algorithm, many different ideas for improvement and optimization came up, but as time is limited, it was impossible to put all ideas into code. Some of the improvements listed here are merely untested ideas, while others are partial solutions to problems not yet solved.

**The trace kernel** could look more than just 1 step ahead. This is not a difficult improvement to implement code-wise, but it will have an impact on execution time.

**Automatic switch of trace kernel.** Since k-3 works well for most patterns, the trade-off in execution time may not justify running k-8 over the whole image. The most noticeable improvement with k-8 over k-3 is when the pattern is curved. This curving occurs mostly near knots. Since the segments provided as input for this method will be knot-free, these curvings will, if they appear, probably be located near the beginning and/or the end of the segment.

**The criteria checks** in the linetrace algorithm can be set to trigger every 2<sup>nd</sup> or maybe even 5<sup>th</sup> pixel instead of every pixel.

**Reducing noise** can be done by automatically determine a cut-off frequency for the initial low-pass filter in the fingerprint algorithm. By finding the line density before calculating the gradient a lot of noise can be suppressed by the low-pass filter. By providing the linetrace algorithm with a cleaner signal, the validation rules can become less strict and the method more robust altogether. Some time was spent analyzing the intensity profile to find the line density, the gradient profile can also be analyzed in an iterative process. Since the profile is merely one pixel wide, an iterative process of low-pass filtering and convolution with sobel operators will be fully viable.

One idea is to filter the gradient profile until a clean frequency is found somewhere near the edges of the board. The highest frequency in the image where the signal is strictly decreasing between local positive maxima and local negative minima will be the highest frequency of lines. This frequency can be used to set the cut-off frequency for a low pass filter, but also to determine the seed points for the linetrace algorithm.

**The method of piecewise segmentation** will introduce new lines at every new restarted trace. Another way to introduce new lines is to, after a normal trace, reverse the direction of the trace (mirror the image around its vertical axis) and trace above the topmost found path, and below the lowest found path. This is easy to implement, and probably very effective.

**The fitting of a polynomial of degree two** in the curve fitting method in chapter 2.2 can reveal pith positions within the board. The polynomial having a global minimum within the board edges can signify the presence of the pith. This method was tested but is at this point not 100% accurate and not used in the algorithm.

**A false edge response** will sometimes appear near each of the board edges. A parameter can be set to decide the size of the margin that keeps the linetrace algorithm from tracing too near the borders. This parameter normally varies between 0-5 pixels. If the margin is set to 5, the trace will never include any of these false lines. True annual lines can appear anywhere on the board, including only a few pixels from the edge. This presents a problem since these lines will not be traced if the margin is set too high. The difference between these false and true lines is that the false lines is a result of the strong edge response of the border, and will go exactly parallel to it. The true lines will go parallel to its closest neighbors. If this distinction is implemented in code, there will be no need for the margin parameter.

**Approximate the amount of late wood.** This improvement is a bigger extension of the algorithm than the ones mentioned above. The negative response in the derivative could be used in conjunction with the positive to find both the transition from late - to early wood (L-E) AND early - to late wood (E-L). Late wood could then be separated from the early wood and a ratio calculated. The hard part will be to approximate the location of the E-L border, but knowing the L-E borders and setting a threshold for the slope based on the response from the 2 nearest L-E borders this should be fully viable.

## 5 References

- [1] Digital Image Processing 2<sup>nd</sup> ed. Rafael C. Gonzales Richard E. Woods Published 2002 by Prentice-Hall Inc.
- [2] Image analysis of annual ring pattern for prediction of wood quality, Per-Johan Sjöberg. Reg nr: LiTH-ISY-EX-3094 2001-01-19
- [3] Kompendium, Bildanalys TSBB07, 2007. Per-Erik Danielsson, Olle Seger, Maria Magnusson Seger, Ingemar Ragnemalm, Department of Electrical Engineering, Linköping University
- [4] MIPS. An image processing program adapted for MATLAB. Developed by the Department of Electrical Engineering, Linköping University and used in some of their image processing courses.  
<http://www.cvl.isy.liu.se/Education/UnderGraduate/TSBB65/download/mips.zip>
- [5] Real-time analysis of the grain on wooden planks, Michael Kellner, Tobias Hanning, Holger Farr. Machine Vision Applications in Industrial Inspection X. Proceedings of SPIE Vol. 4664(2002)
- [6] Timber: Its nature and behaviour 2<sup>nd</sup> ed., J.M Dinwoodie, Published 2000 by E & FN Spon
- [7] WoodEye Training manual, User Guide WoodEye ver. 7.0, printed 2005
- [8] [http://www.atb-technology.de/frontal\\_engl.html](http://www.atb-technology.de/frontal_engl.html)
- [9] [http://www.sprecher-automation.com/upload/graphics/PDF/SWA/SPRESCAN\\_RING\\_12310129enE.pdf](http://www.sprecher-automation.com/upload/graphics/PDF/SWA/SPRESCAN_RING_12310129enE.pdf)
- [10] <http://www.woodeye.se/>

## Appendix

### *The trace kernel test*

Board	Column start/stop	sno	Lines on board	k-8		k-3		Comment
				Lines missed	Extra lines	Lines missed	Extra lines	
4	2400/3000	0	19	2		2		
4	2400/3000	1		1		1		line missed near edge
4	2400/3000	2		1		1		line missed near edge
4	2400/3000	3		1		1		line missed near edge
4	2400/3000	4		3		3		line missed near edge
4	2400/3000	5		4		4		
4	6400/7000	0	21	2		2		line missed near edge
4	6400/7000	1		2		2		
4	6400/7000	2		2		2		
4	6400/7000	3		2		2		
4	6400/7000	4		2		2		
4	6400/7000	5		3		3		
1	4100/4700	0	5	2		2		line not parallel
1	4100/4700	1		1		1		line not parallel
1	4100/4700	2		1		1		
1	4100/4700	3		1		1		complications by lower line
1	4100/4700	4		1		1		
1	4100/4700	5		1		1		
1	4100/4700	6		1		1		
1	4100/4700	7		1		1		
1	4100/4700	8		1		1		
1	4100/4700	9		1		1		
1	4100/4700	10		1		1		
1	4100/4700	11		1		1		
1	4100/4700	12		2		2		
1	6900/7200	0	5	0		0		possible rot
1	6900/7200	1		0		0		
1	6900/7200	2		1		1		
1	6900/7200	3		1	1	1	1	

1	6900/7200	4		2	1	2	1	
1	6900/7200	5		2		2		
3	1850/2300	0	24	2		2		waviness in the image complicates tracing
3	1850/2300	1		5		5		
3	1850/2300	2		6		6		
3	6500/6900	0	24	5		5		
3	6500/6900	1		4		4		
3	6500/6900	2		6		6		
3	6500/6900	3		8		8		
3	6500/6900	4		9		9		
4	6500/6900	0	22	1		1		line coming in from the border
4	6500/6900	1		2		2		
4	6500/6900	2		1		1		
4	6500/6900	3		2		2		
4	6500/6900	4		2		2		
4	6500/6900	5		4		4		
4	650/1100	0	19	1		1		line missed near lower edge
4	650/1100	1		1		1		
4	650/1100	2		1		1		
4	650/1100	3		1		1		
4	650/1100	4		1		1		
4	650/1100	5		1		1		
Board	Column start/stop	sno	Lines on board	Lines missed	Extra lines	Lines missed	Extra lines	Comment

### *The growth direction estimation test*

The green cells indicate a correct estimation while the red cells indicate an incorrect estimation. If the pith is present in the board, lines with both growth directions will be present and the cell is uncolored. The presence of the pith is indicated by the declaration of both directions in the “Actual direction” column, with the more dominant direction appearing first. A result including the acronym “pd” means that the presence of a pith was detected. All the methods tested are described in chapter 2.2, except the Curve fitting (low-pass) method. This is the same method as the quadratic curve fitting with the exception that the profile is low-pass filtered.

Board	Sampled column	Actual direction	Number of lines	Derivative pixel count	Line width estimation	Curve fitting (quadratic)	Curve fitting (linear)	Curve fitting (low-pass)	Comment
1	1330	1	6	0	1	1	1	1	weak contrast
	5200	1+0	6	0	1	0	0	1	pith
	6800	1	5	1	1	1	1	1	ok contrast
	8200	1+0	6	1	1	1	1	1	good contrast, pith
2	2900	1	~60	0	1	0	0	1	extremely high line density
	5100	1	~60	0	1	1	1	1	extremely high line density
	11000	1	~60	1	1	1	1	1	extremely high line density
3	2000	1	25	1	1	1	1	1	ok contrast, high line density
	12100	1	24	1	1	1	1	1	good contrast
	13000	1	20	1	1	1	1	1	good contrast
4	900	1	19	1	1	1	1	1	good contrast
	5200	1	21	1	1	1	1	1	good contrast
	13600	1	26	1	1	1	1	1	good contrast
5	750	0+1	4	0	0	0 (pd)	0	0	good contrast, pith
	3300	0+1	6	1	1	1 (pd)	1	1 (pd)	good contrast, pith
	10150	1+0	11	0	1	1 (pd)	1	1 (pd)	good contrast, pith
	12230	1+0	8	1	1	1	1	1	good contrast, pith
6	6100	1+0	5	1	1	1	1	1	weak contrast
	6800	1+0	7	0	1	0 (pd)	0	0	weak contrast, pith
	8500	1+0	4	0	1	0 (pd)	0	0 (pd)	weak contrast, pith
	10000	1+0	5	1	1	0 (pd)	0	0	weak contrast, pith
7	700	1	5	1	1	1	1	1	ok contrast
	4200	1	4	0	1	1	1	1	ok contrast
	6700	1	6	1	1	1	1	1	good contrast
	9650	1	5	1	1	1	1	1	good contrast
	13000	1	7	1	1	1 (pd)	1	1 (pd)	good contrast
8	700	0	13	0	0	0	0	1	optimal contrast
	10500	0	11	0	0	0 (pd)	0	0	optimal contrast
	13500	0	16	0	0	0 (pd)	0	0	good contrast, area of weak contrast
9	1050	1	23	0	1	1	1	1	weak contrast
	4600	1	17	1	1	1 (pd)	1	1	good contrast. Mixed ratio of late wood
	8200	1	20	1	1	1	1	1	good contrast. Mixed ratio of late wood
	12200	1	5,5	1	1	1	1	1	weak contrast
10	2400	1	5,4	1	1	1 (pd)	1	1 (pd)	weak contrast, discoloration

	7000	1	5,3	0	1	1	1	1	ok contrast. Mixed ratio of late wood
	12800	1	5,2	1	1	1	1	1	weak contrast, discoloration
Board	Sampled column	Actual direction	Number of lines	Derivative pixel count	Line width estimation	Curve fitting (quadratic)	Curve fitting (linear)	Curve fitting (low-pass)	Comment

### *The sensor comparison test*

When there is a difference in performance between the blue channel (B) and the grayscale (G) material, the worse result is marked with red. The comments about missed lines near the lower edge is due to an edge margin that is set to avoid false lines that can appear near the board edges, but this will also exclude true lines within that margin. Decreasing that margin would reduce the number of lines missed in this test. A way to distinguish these false lines from true lines is discussed in chapter 4.1. With such a method, there would be no need to set a margin.

Sensor	Board	Column	Lines on board	Lines missed	Extra lines	Comment
B	1	1100	6	0	2	1 false line, hard to detect as false. Very weak contrast
G	1		6	0	1	very weak contrast
B	1	3010	4	0	0	good contrast
G	1		4	0	0	good contrast
B	1	4090	5	0	0	good contrast
G	1		5	0	0	good contrast
B	1	6820	5	0	0	good contrast
G	1		5	0	0	
B	1	9630	6	1	0	missed line near bottom edge, ok contrast
G	1		6	1	0	missed line near bottom edge, ok contrast
B	2	2310	~50	29	0	extremely high line density, very weak contrast
G	2		~50	39	0	extremely high line density, very weak contrast
B	2	11000	27	4	0	high line density, very weak contrast



G	2		27	20	0	high line density, very weak contrast
B	2	12100	25	2	0	extremely high line density, weak contrast
G	2		25	13	1	extremely high line density, weak contrast
B	2	1880	24	2	0	high line density, good contrast
G	3		24	3	0	high line density, good contrast
B	3	5050	20	1	0	ok contrast
G	3		20	3	0	ok contrast
B	3	6670	24	1	0	missed line near lower edge (high density), good contrast
G	3		24	2	0	missed line near lower edge (high density), good contrast
B	3	11950	17	1	0	missed line near lower edge (high density), good contrast
G	3		17	1	0	missed line near lower edge (high density), good contrast
B	3	12900	21	3	0	missed lines near lower edge (high density), good contrast
G	3		21	4	0	missed lines near lower edge (high density), good contrast
B	4	2100	19	0	0	ok contrast
G	4		19	0	0	ok contrast
B	4	3800	19	1	0	missed near bottom edge, good contrast
G	4		19	1	0	missed near bottom edge, good contrast
B	4	5200	21	1	0	missed near bottom edge, good contrast
G	4		21	1	0	missed near bottom edge, good contrast
B	4	8700	24	1	0	missed near bottom edge, good contrast
G	4		24	1	0	missed near bottom edge, good contrast
Sensor	Board	Column	Lines on board	Lines missed	Extra lines	Comment